LUND
UNIVERSITY

Dry Coating Technology for Lithium-ion Battery Electrode Fabrication

Master Thesis

Can Yao

2024

Department of Energy Science

Faculty of Engineering, LTH, Lund University

This research is covered by a confidentiality agreement.

Parts of the parameters and details will not be disclosed.

Supervisor: Xuesong Bai

(xue-song.bai@energy.lth.se)

Co-supervisor: Jinhua Sun

(jinhua@chalmers.se)

Examiner: Hesameddin Fatehi

(hesameddin.fatehi@energy.lth.se)

MSc Thesis

Department of Energy Science

Faculty of Engineering, LTH

Lund University

Box 117, 221 00 Lund

Sweden

ISRN LUTMDN/TMHP-24/5583-SE

ISSN 0282-1990

Abstract

With the vigorous development of the electric vehicle industry, there is an increasing demand for high-capacity, high-stability batteries, and higher requirements are also placed on clean, non-toxic, and efficient battery production processes. The electrode is one of the most important components in lithium-ion batteries. It determines the capacity and overall performance of the battery. The fabrication process of electrodes mainly involves several steps, among which the coating process refers to the process of evenly spreading the active material on the current collector. In the conventional electrode fabrication process, the wet coating method is used. It involves toxic NMP solvents and the drying process would take a lot of time which is unfavorable and limits the electrode production. In recent years, a new approach is gradually making its way onto the scene. Dry coating technology, as an emerging fabrication process for lithium-ion batteries, with the merits of reducing energy consumption, reducing manufacturing cost, increasing production speed and capability of producing clean, high-capacity electrodes, is gradually attracting more and more attention. However, PTFE fibrillation and electrostatic spraying currently dominate the market, which places a high requirement for processing equipment and operating environment. There is a lack of efficient and economical coating technology to lower the operational barriers for the large-scale promotion of this technology. In this thesis, a simple and highly efficient coating method for dry coating technology is successfully designed and fabricated. Through the comparison of the LFP, NMC, and LFP/NMC blended electrodes prepared by the wet coating and the dry coating methods, it is proved to be a useful and promising method in the future.

Popular Science Summary

Have you ever considered buying an electric car? What do you think is most appealing to you or what is holding you back from buying one? One thing that most people will be concerned about for sure: battery range. In an electric car, the battery is one of the most important components as it is the power source for the entire vehicle, while the key to determining battery performance is the electrode material inside, which affects the range capacity and charging speed. The commercially available electrode materials on the market include LFP, known for its stability, and NMC811, recognized for its high capacity. Electric vehicle fires are also a major safety concern that plagues many people who want to purchase electric vehicles. Batteries using LFP materials have higher thermal stability, while batteries using NMC materials have lower ignition temperatures and are more prone to fire. Therefore, whether it is possible to directly mix the two to obtain an electrode that not only has a high capacity but also demonstrates high stability is a question in this study.

The pollution and recycling of lithium-ion batteries is another important topic, as many of the world's leading battery companies have announced that they will begin to increase their investment in the production of cleaner and greener batteries. In the conventional lithium-ion battery electrode preparation process, wet coating technology is widely used. Coating means depositing the electrode active material, such as LFP, on a conductive aluminum or copper foil. However, the wet coating process requires the use of the toxic NMP solvent, which poses significant environmental and health risks and creates a lot of trouble for subsequent solvent recovery and treatment. In recent years, dry coating process technology has gradually become the focus of research because it doesn't involve the usage of any toxic solvents. However, solid particles and liquids have different properties. Liquids can be easily spread on aluminum foil, while it is difficult to achieve uniform powder deposition for solid particles The current mainstream technologies, such as electrostatic spraying, require very sophisticated instruments and an extremely dust-free working environment, which is not conducive to the promotion of

this technology. Thus, another focus of this article is to develop a novel coating technique for rapid and efficient dry coating deposition. The experimental results prove that the developed serrated blade can efficiently realize the deposition of solid particles and a thin film with good uniformity. The performance of batteries prepared by the two processes was tested, and the results showed that the dry coating process exhibited performance equal to or even better than the wet coating process. This demonstrates the great potential of the dry coating process. Meanwhile, the results also show that the combination (blending) of LFP and NMC materials is not a good strategy.

Acknowledgments

Many gains from this short six months. I would say thanks to everyone I met during my study life. I would like to thank my supervisor Prof. Sun at Chalmers University of Technology, who gave me valuable advice and directions during this thesis. Thanks to Prof. Bai who is my supervisor in LTH. He is a nice and kind professor who always treats his students well. Thanks to my examiner Prof. Hesam, he is really responsible and good at teaching. His questions are critical and in-depth which I like them much. I would also like to thank my friends at the Graphene Lab at Chalmers University of Technology. Thanks to Tianlin for his guidance on the entire dry coating process. He contributed greatly to leading me to familiarize myself with the lab operations. Thanks to Ruiqi, he is a hardworking and friendly person and helps me a lot. Thank you Jonny for your unparalleled technical support. Lastly, I want to thank myself for my perseverance and courage to overcome all kinds of problems these months. Special thanks to my parents, I wouldn't have gotten this far without their support.

I spent the best two years of my life at Lund University. Those lovely, vivid days, those interesting and kind friends, those free and floating feelings, I shall always keep in my heart and never forget. Although we come from different corners of the world, with different colors, ages, and cultures, we all share a common vision: a commitment to contribute to a better future.

Ever since I graduated from XMUM, I've thought very clearly about my life. How should I spend my life? What kind of person do I want to be? "*Pursue Excellence, Strive for Perfection*." This school motto energies me with infinite power. I will take this motto to find my path through relentless seeking in the future. Knowledge is endless, Love is boundless.

"路漫漫其修远兮，吾将上下而求索。"

"The journey ahead is long and far-reaching; I will seek high and low to find my way."

Table of Contents

List of Figures

Abbreviations

Cyclic Voltammetry (CV)

Dimethyl Carbonate (DMC)

Ethylene Carbonate (EC)

Graphene Oxide (GO)

Lithium Cobalt Oxide (LCO)

Lithium Hexafluorophosphate ($LiPF_6$)

Lithium Iron Phosphate (LFP)

Lithium Manganese Oxide (LMO)

Lithium Nickel Manganese Cobalt Oxide (NMC)

Lithium-ion Battery (LIB)

N-Methyl-2-pyrrolidone (NMP)

Polytetrafluoroethylene (PTFE)

Polyvinylidene Fluoride (PVDF)

Reduced Graphene Oxide (rGO)

Scanning Electron Microscopy (SEM)

1. Introduction

1.1 Problem Description

Ever since 1958 when Harris studied the action of lithium ions in different organic electrolytic solutions, until 1991, when Sony introduced the first commercial lithium-ion battery, research on lithium-ion batteries has attracted more and more attention worldwide (Reddy *et al.*, 2020). In recent years, under the background of carbon neutrality, the electric vehicle market has been exceptionally developing with numerous investments from headline technology companies and government institutes constantly flowing in. As the pivotal component in an electric vehicle, batteries, known as the heart of the power system, are getting more and more focused. Battery technology represented by lithium-ion batteries, has been strongly driven by the booming development of the electric vehicle market. Research on lithium-ion batteries has become extremely popular. The energy density of lithium-ion batteries has seen massive and rapid development, from 80 Wh/kg in the early days to 280 Wh/kg commercially available today (Khan *et al.*, 2023). Still, it moves towards higher energy density through advanced materials and strategies like silicon-carbon anode, high-energy density electrolytes, lithium-sulfur batteries, and all-solid-state batteries.

To address the range anxiety in electric vehicles, high-capacity batteries are the key to the problem. In lithium-ion batteries, the electrode material is a key factor in determining capacity. The current research mainly focuses on cathode materials. This is due to the fact that while the typical graphite anode boasts a theoretical capacity of 372 mAh/g, cathode materials normally deliver a specific capacity of around 200 mAh/g (Nitta *et al.*, 2015). The theoretical capacity here refers to the maximum electron numbers that can be provided assuming that all lithium ions in the material participate in the electrochemical reaction, which is calculated through Faraday's first law, and specific capacity is the capacity per unit mass of the material. Active materials with higher specific capacities are still being explored.

On the other hand, the explosive development of the electric vehicle market puts higher demands on the production speed of electrodes. Wet coating technology is widely used in conventional electrode manufacturing, which takes up a large amount of production area and requires a lot of time for electrode drying (Zhang *et al.*, 2021). This is obviously not conducive to the cost control of commercial companies. More importantly, in the wet coating process, the toxic volatile solvent N-Methyl-2-pyrrolidone (NMP) needs to be introduced to dissolve the active materials, binders, and conductive additives to form a uniform solution (Bouguern *et al.*, 2024). This imposes requirements on subsequent post-processing such as solvent recovery. Environmentally friendly, non-toxic, efficient, and sustainable processing techniques need to be researched.

The dry coating process can be seen as a potential and feasible solution (Ludwig *et al.*, 2016a). The dry coating process eliminates the use of any solvent during the entire process, thereby avoiding the use of the toxic solvent NMP. This technology enables a notable decrease in plant floor space requirements, personnel costs and energy consumption, and is estimated to save at least 20% of electrode production costs (Gyulai, Bauer and Ehrenberg, 2023). While the traditional wet coating method is well established, the dry coating method, as an emerging technology, currently has many uncharted territories to explore. At present, some companies and scientific research institutions have been able to produce effective dry coating electrodes, which has verified the feasibility of this technology. However, details about the technology are protected by copyright and need to be explored in more depth. And how the technology can be widely applied to commercial manufacturing is also another important challenge. Furthermore, dry coating technology has already been applied in industrial production to some extent, but how innovations can be made to achieve some breakthroughs that cannot be solved as before is another question. For example, how to achieve high-performance (stability and capacity) electrode preparation through the structural design of the electrode for the dry coating process.

1.2 Aim of the Research

This study aims to investigate the feasibility and potential of the dry coating process and find a simple and efficient coating method for electrode production.

1.3 Research Questions

1. How to design a simple method to efficiently and uniformly coat electrode materials onto current collectors?
2. Compared with the conventional wet coating method, is the battery produced by the dry coating method showing better performance?
3. How to prepare high-performance lithium-ion batteries by dry coating technology through a series of innovations like structure design and material adjustments?

1.4 Delimitations

This research centers on the dry coating process for lithium battery electrode fabrication. The wet coating technology is only used as a reference group for comparison and is not specifically studied. The study focuses on electrode materials used in lithium batteries, particularly emphasizing positive electrode materials. Other components in the lithium-ion battery, such as electrolyte, separator, and current collector, remain the same and are not specifically studied. The study will choose a half-cell, which uses Li metal as the counter electrode (negative electrode) to study the properties of the positive electrode materials. The internal structure of the electrode materials will be designed, but the basic structure of the entire lithium-ion battery will not be changed. The assembled battery structure is a coin cell. Other common battery shell structures such as cylindrical cells, prismatic cells and pouch cells are not within the scope of the study. For battery performance testing, operating voltage, cycle numbers, and specific capacity are examined, while the aging and thermal stability of the battery is not under study.

2. Background

2.1 Structure of Lithium-ion Batteries

A basic battery cell consists of two electrodes (positive and negative), electrolytes, and a separator (as shown in **Figure 1**). The working principle of lithium-ion batteries is the chemical potential generated by the redox reaction between two electrodes promotes the intercalation or deintercalation of lithium ions between the two electrodes. The redox reaction here refers to the general term for oxidation reaction and reduction reaction, which take place on each side of the electrode (if oxidation occurs on one side, reduction occurs on the other). Intercalation and deintercalation are terms in electrochemistry that describe the movement of lithium ions. Intercalation refers to the process where lithium ions enter and bind to specific sites within the crystal lattice of the electrode material, while deintercalation refers to the process where lithium ions leave these sites. Lithium ions migrate in the electrolyte under the chemical concentration gradient and electric field gradient, while the electrons are collected by the current collector at the electrode (usually the positive electrode is aluminum foil and the negative electrode is copper foil) and flow to the external circuit (Schalenbach *et al.*, 2023).

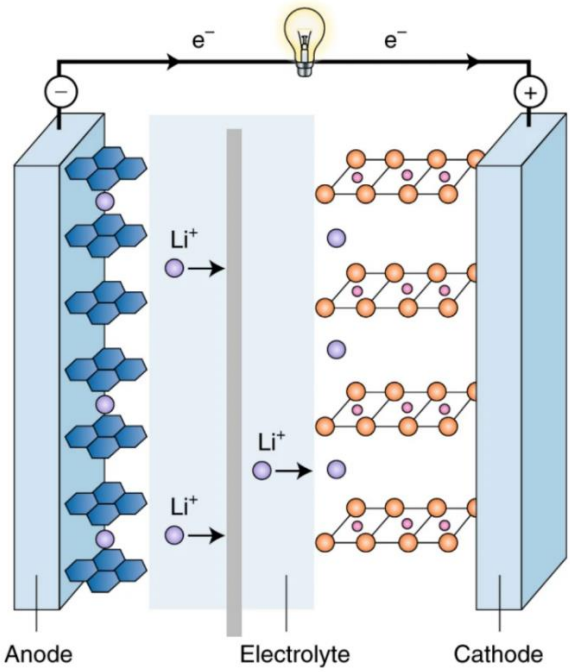

Figure 9: Cell structure of a lithium-ion battery (Goodenough, 2018).

2.2 Components within a Lithium-ion Battery

2.2.1 Positive Electrode Materials

The positive electrode, (also called the cathode during the discharge process), is the terminal with the higher potential in the discharging process and is also where the reduction reaction occurs. Cathode materials generally require high conductivity, high diffusion coefficient, good stability, and low cost. Common cathode materials are Lithium Iron Phosphate ($LiFePO_4$, LFP), ($LiNi_xMn_yCo_{1-x-y}O_2$, NMC), Lithium Cobalt Oxide ($LiCoO_2$, LCO), and Lithium Manganese Oxide ($LiMn_2O_4$, LMO**)** (Hebert and Mccalla, 2021). And batteries are usually named according to the positive electrode material used. Typically, LFP and NMC batteries are the most commonly used power batteries in commercial electric vehicles nowadays, not only due to their high energy density and stability, but also attributed to their availability and cost efficiency. LFP batteries are renowned for their outstanding thermal stability and cost-effectiveness; however, their specific capacity is only 170 mAh/g, significantly lower than the 200 mAh/g of NMC batteries (Chandra *et al.*, 2023). NMC batteries are favored by more and more electric vehicle manufacturers for high-end vehicles, most importantly because they can provide excellent energy density and effectively alleviate range anxiety. The chemical formula of the positive electrode material for NMC batteries is $LiNi_xMn_yCo_{1-x-y}O_2$, where the ratio of its components (Ni, Mn, Co) can be regulated to obtain different battery performance like normally NMC111, NMC532, NMC622, NMC811. For instance, in NMC811, the proportions of its components Ni: Mn: Co are indicated by the numbers 8:1:1. In general, the content of Ni ions determines the energy density as well as the capacity of the battery, whereas Co ions primarily contribute to stabilizing the electrode structure (Aryal *et al.*, 2021; Liu *et al.*, 2021). The role of Mn ions remains researched, with some scholars suggesting their potential to enhance battery stability and rate capability, although a consensus has yet to be reached (Thapa *et al.*, 2022). The study of high-nickel NMC batteries is getting more and more attention due to their potential to offer greater energy density and decrease reliance on costly cobalt. However, the current research on batteries using lithium as the cathode material tends to be capped, and

some research on alternative solutions like sodium-ion batteries is ongoing because they are more cost-effective (Kotobuki, Yan and Lu, 2023).

2.2.2 Negative Electrode Materials

The negative electrode, (also called the anode during the discharge process), is the electron donor and gives electrons to the positive electrode when an oxidation reaction occurs. Carbon-based materials represented by graphite are widely used as negative electrode materials due to their lightweight, high conductivity, low cost, and low electrode potential (Zhang *et al.*, 2021). In addition to this, other carbon materials, including carbon black, carbon nanotubes (1D materials), as well as 2D materials like graphene, graphene oxide (GO), and reduced graphene oxide (rGO) have also been introduced for use as negative electrode materials (Deng *et al.*, 2022). These carbon-type materials provide excellent specific surface area and sufficient sites for the intercalation of lithium ions. However, the lower theoretical capacity of graphite (372 mAh/g) and the property of capacity decay due to the consumption of Li ions in the first cycle have prompted more research on alternative materials (Asenbauer *et al.*, 2020). Silicon materials can offer unrivaled high energy density (3579 mAh/g), but the huge volume expansion (300%) caused by the lithium deintercalation process, which renders the failure of the cell structure, and the capacity degradation caused by reversible lithium depletion, raises some challenges (Hossain *et al.*, 2023).

2.3 Fabrication Process of Electrodes

2.3.1 Conventional Wet Coating Method

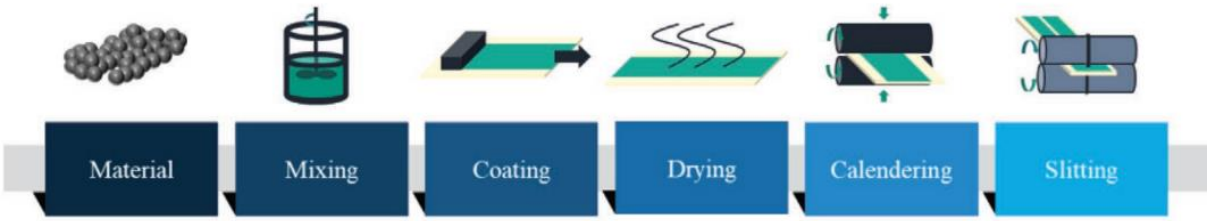

Figure 10: Electrode fabrication process through conventional wet coating (Fichtner *et al.*, 2021).

The wet coating process is still the most widely used technology in the industry. As shown in **Figure 2**, the manufacture of electrodes from raw material to final product generally involves these steps:

1. Material Preparation: Raw materials can be purchased directly from specialized manufacturers or obtained through experimental synthesis. The performance of the final electrode is directly influenced by the purity of the raw material, the particle size, and their physical and chemical properties.
2. Mixing: Electrode active materials, binders, conductive additives, and solvents are mixed in certain proportions. Commercial manufacturing typically employs planetary mixers for slurry mixing. Additionally, pre-treating the material before mixing is possible, such as ball milling or grinding to achieve finer particles. It's important to note that the mixing sequence can have an impact on the final properties, and simultaneously mixing may result in uneven dispersion of materials (Wang *et al.*, 2020).
3. Coating: After all the materials are mixed, the sample presents a relatively viscous liquid. At this time, a coating machine (slot die coating or doctor blade coating) is generally used to spread the material evenly on the current collector (copper foil or aluminum foil) (Reynolds *et al.*, 2021). The coating process significantly affects the thickness of the

electrode film. And high-performance lithium-ion batteries demand stringent requirements for the uniformity of film formation, as it directly influences the pathway for lithium-ion transmission and the consistency of the reaction.

4. Drying: The drying process is the most problematic and critical part of the electrode manufacturing process. It is also one of the most energy-intensive and time-consuming steps during the entire electrode manufacturing process (Zhao *et al.*, 2023). The purpose of drying is to eliminate the moisture as well as the toxic solvent NMP from the slurry. There have been many studies on drying rates, temperatures, and methods, but the inconsistency of coatings after drying, migration of binders, and microstructural defects such as cracking and flaking have not yet been fully resolved (Zhang *et al.*, 2022).
5. Calendering: Calendering is another crucial step aimed at enhancing electrode uniformity by reducing thickness variations and minimizing porosity to achieve a denser electrode structure. The most common is the roll-to-roll calendering machine. The electrode material passes through the gap between the two rollers and becomes denser under the action of pressure. The thickness and density of the electrode can be controlled by adjusting the gap and pressure.
6. Cutting: In the final stage, the electrode sheets are cut to the desired dimensions using die-cutting or laser-cutting methods. Precision in cutting is essential to ensure regular edges without burrs, as any imperfections can potentially puncture the separator, leading to short circuits.

2.3.2 Advanced Dry Coating Method

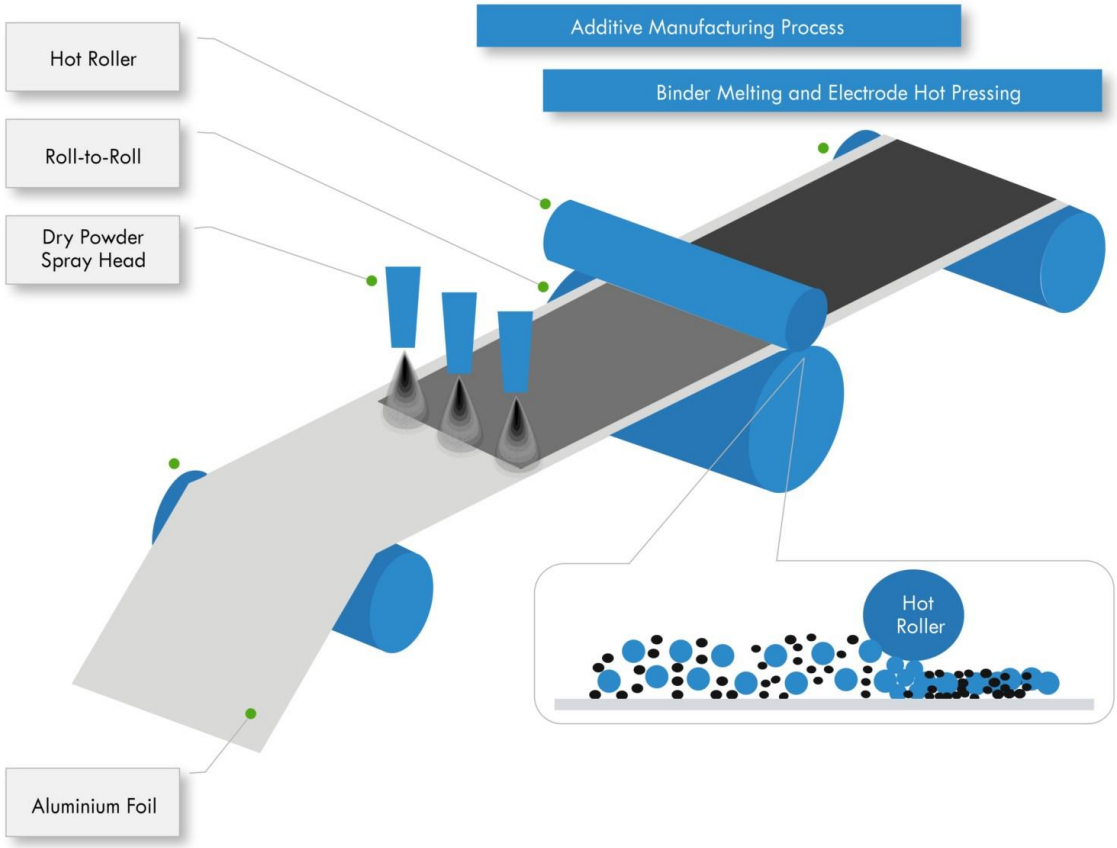

Figure 11: Schematic diagram of the dry coating method for electrode fabrication process (Morris, 2023).

The dry coating process is an emerging electrode processing technology without using any solvents during the entire process (see **Figure 3**). After stirring and mixing, solid powders such as electrode active materials, binders and conductive additives are directly coated and deposited on the current collector, and then sent to a roll-to-roll calendering machine for pressing. This technology first originated from supercapacitors and was later promoted and applied to lithium-ion battery technology. Maxwell Technology, a well-known company famous for some technology patents in dry coating electrodes, was acquired by Tesla in 2019, primarily for its pioneering invention of the extensively utilized PTFE fibrillation method in dry electrode processing (Lienert, 2023). Recognizing the potential of this breakthrough technology, numerous companies have since ventured into related research and development efforts.

Volkswagen, in collaboration with its partner Koenig & Bauer, has announced their successful mastery of the technology. If implemented on a large scale, this advancement could potentially slash battery production costs by hundreds of millions of euros annually (Waldersee, 2023). The Fraunhofer Institute also stated that they have successfully produced environmentally friendly and cost-effective dry coating technology. Compared with the traditional wet coating process, dry coating can easily produce thicker electrodes with higher energy density and significantly reduce cracking due to drying. The absence of solvents simplifies the processing steps considerably and not only reduces energy dependence but also increases the number of parts processed per unit of time. It also eliminates the need to consider the recycling of toxic solvents. It is reported that the dry coating method can save around 50% of energy consumption and about 20% of the total battery manufacturing cost (Yao *et al.*, 2023).

In short conclusion, it has these merits compared with the wet coating method:

- Lower energy consumption;
- Lower manufacturing cost;
- More efficient production speed;
- Thicker electrodes can be prepared;
- Compatible with all-solid-state batteries;
- More environmental-friendly without any toxic solvents.

But it doesn’t mean that it’s perfect, meanwhile, it accompanies some drawbacks:

- Weaker adhesion;
- Difficult to achieve uniform coating;
- Hard to prepare thin electrodes;
- Lower maturity brings more uncertainty;
- Sophisticated equipment and strict coating process control is required.

2.3.3 Coating Methods for Dry Coating

Polymer Fibrillation

Polymer fibrillation is the most representative method of dry coating technology, which originated from Maxwell Technology Company. The recipe of this technology is to use polymer molecules PTFE (Polytetrafluoroethylene) to fibrate under high shear force to form elongated fibers that wrap the active material and produce a binding effect (Wang *et al.*, 2023). The key to this method is how to generate fibrillation of the polymer molecules, which is typically done using a high-speed air-flow pulverizer that generates linear, high-shear forces to stretch the molecules (as shown in **Figure 4**). The diameter of these fibers is between 1μm and 10 nm, which can completely wrap the active material particles like a fishing net. This mesh structure can work well as a support to form a self-supporting membrane for the electrode.

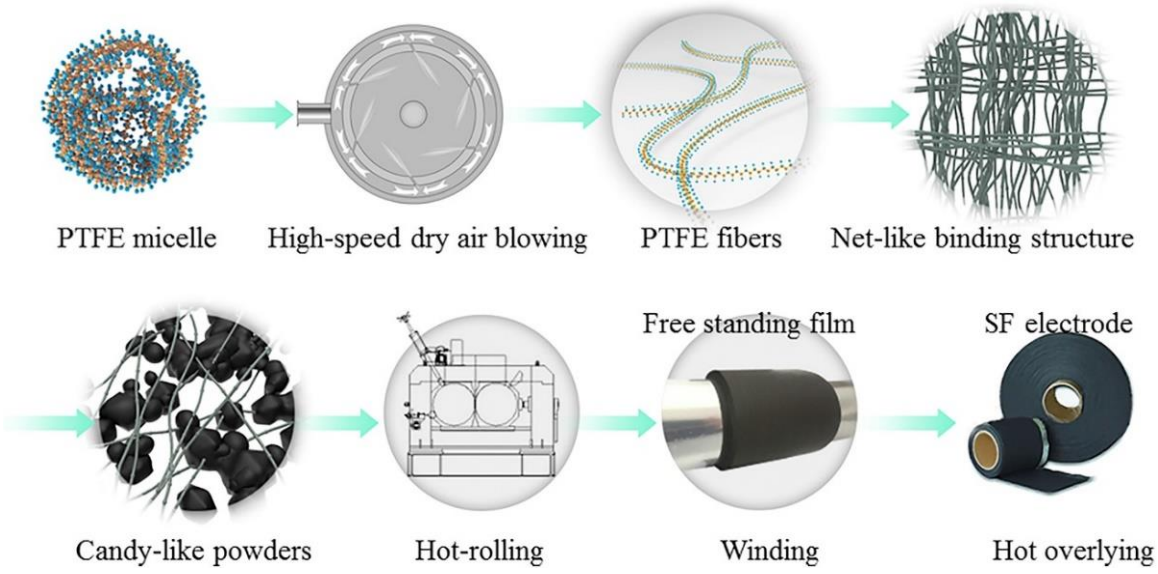

Figure 12: Process of PTFE fibrillation, from micelle to mesh structure (Zhou *et al.*, 2020).

Generally, Polyvinylidene fluoride (PVDF) is widely used as the binder in conventional wet coating due to its good thermal stability, high mechanical strength, and chemical inertness (Dallaev *et al.*, 2022). However, due to the orientation of the molecules, it is difficult to achieve a fibrillation process similar to PTFE. This distinction results in a different binding mechanism

compared to that of PTFE fiber (see **Figure 5**). The benefit of PTFE fibrillation is that it can control the size of the fibers by adjusting the shear force and the speed of the airflow. Therefore, if the fibers are sufficiently fine, only a small amount of binder content is needed to achieve a good binding. Reducing the amount of binder is very helpful for the performance of the battery as it frees up more space for the active materials and conductive agents, increasing the capacity and conductivity of the electrodes. Simultaneously, this mesh structure can offer increased contact sites, thereby facilitating a stronger binding effect. Conventional PVDF, on the other hand, has difficulty in dispersing the particles, causing some of the particles to agglomerate together, and these excess particles can even block ionic transport, resulting in a reduction in the material's performance.

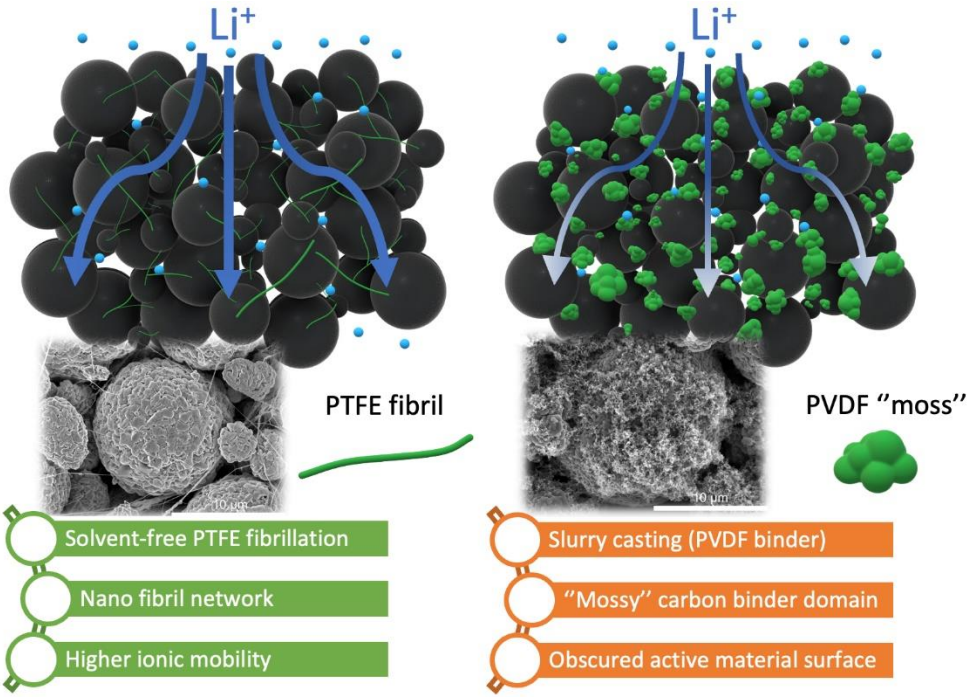

Figure 13: Illustration of the binding mechanism of PTFE fibril and pristine PVDF (Matthews *et al.*, 2024).

Electrostatic Spraying

Electrostatic spraying is currently the most promising coating technology because it can control the size of coating particles and the thickness of the film and get a relatively uniform electrode film. The devices involved are shown in **Figure 6**. First, the spray gun charges the fluidized

particles when charging while the current collector is grounded. In a dust-free environment, dry particles are ejected by the airflow and deposited on the surface of the current collector under the action of the electric field (Ludwig *et al.*, 2016). Grounding serves not only to create a potential difference but also to absorb excess charge. Through electrostatic spraying, very fine control of the electrode film can be achieved, including the production of very thin electrodes. But what follows is strict requirements for both equipment and production environment. This is because electrostatic spraying requires not only high-precision spray guns and complex electrical deposition equipment, but also a highly dust-free workshop. Additionally, it not only demands accurate monitor to detect the uniformity of electrode film, but the slow motion of spray gun requires more time for production, which slows down the production progress.

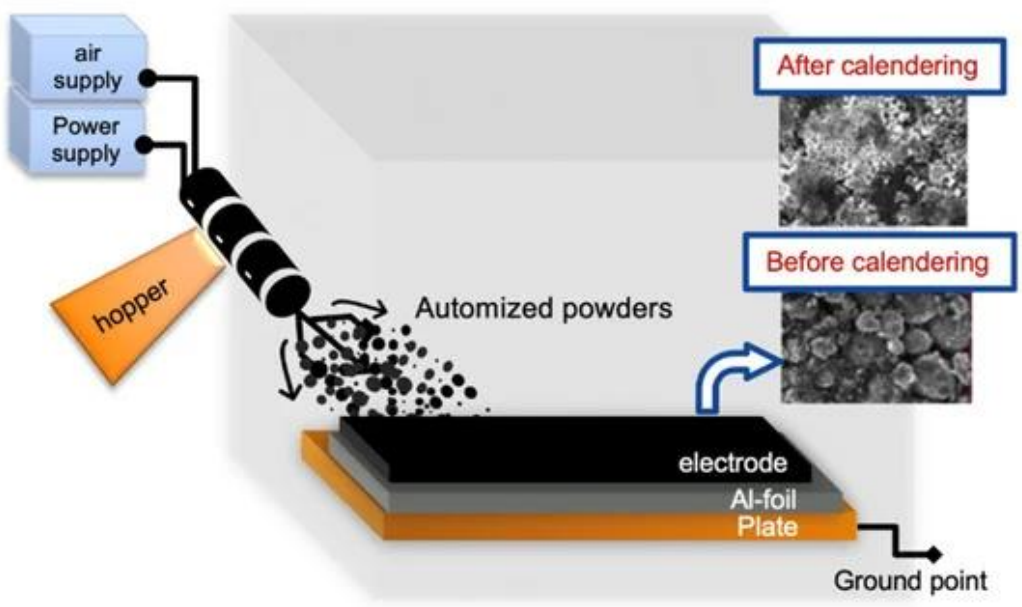

Figure 14: Schematic diagram of electrostatic spraying device (Bryntesen *et al.*, 2021).

Hot Pressing

In the wet coating process, the liquid material is generally coated using the slot-die or doctor-blade method, as shown in **Figure 7**. The thickness of the coating ranges from a few microns to several hundred microns (Kamarulzaman *et al.*, 2020; Huang *et al.*, 2024). These methods,

as well as methods such as spin-coating, are also widely used in the field of solar cells. However, they can only be applied for liquids with a certain viscosity and not for solid particles. This is because solid particles tend to collide with each other and have strong friction, and eventual dispersion.

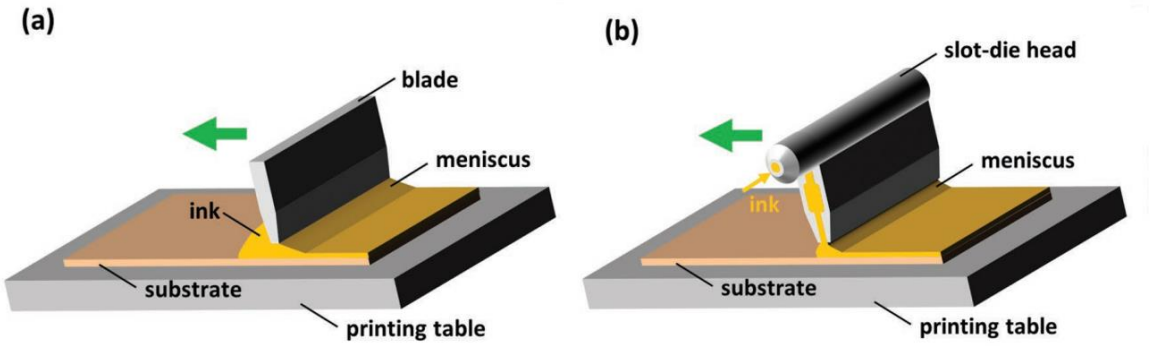

Figure 15: Blade coating and Slot-die coating used in wet coating method (Howard *et al.*, 2019).

The most simple and straightforward coating process is depositing solid particles through direct pressing. In order to apply the same pressure to each part and to ensure uniformity of film formation, a template is generally used as a substrate. By hot pressing, the surface of the electrode can be made flatter and denser. The applied temperature also causes the binder to thermally fuse, resulting in better dispersion and binding. Ryu et al. reported a dry coating process for electrodes with ultra-high loadings (see **Figure 8**). They first etched the aluminum foil current collector to create submicron pores, which can effectively increase the contact interface between the electrode and the current collector, enhancing charge transmission and adhesion. They then placed the electrode material into the template for hot pressing, with the temperature set to 180°C. Finally, they successfully fabricated an electrode with a load of up to 17.6 mAh cm^{-2} and a specific energy density of 360 Wh kg^{-1}. And the performance of the prepared dry coating electrodes is better than that of the wet coating electrodes (Ryu *et al.*, 2023).

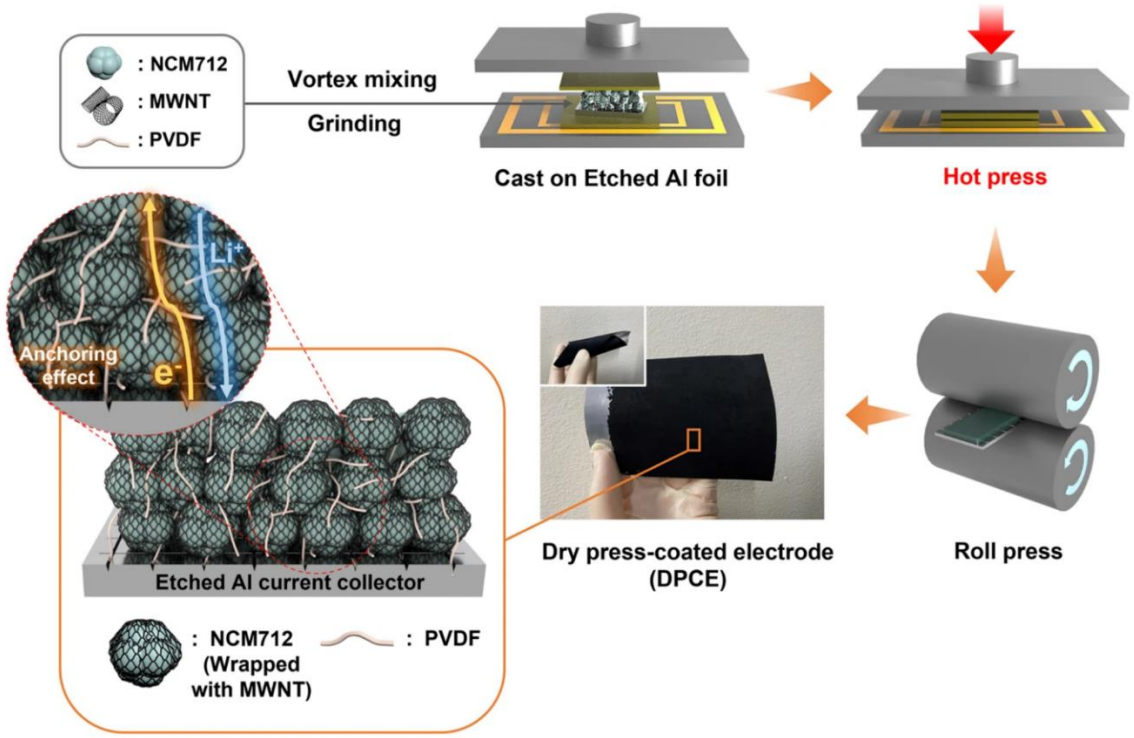

Figure 16: Schematic diagram of the hot pressing process (Ryu *et al.*, 2023).

2.4 Basic Structure of Electrodes

In order to obtain an electrode with excellent chemical reactivity, good stability, high energy density, and high conductivity, it is necessary to in-depth design the microstructure of the electrode. In a basic electrode structure, there are two contact interfaces. First is the contact interface between the current collector and the electrode material layer which consists of active material, conductive additive and binder (see **Figure 17**).

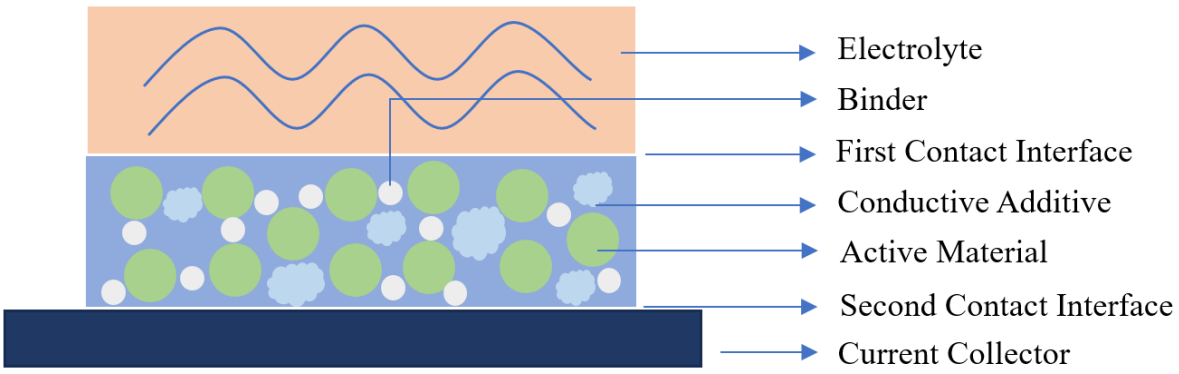

Figure 9: Schematic diagram of electrode structure.

This contact interface primarily serves to conduct electrical charge. Electrodes with high conductivity and low chemical impedance are able to quickly transfer the charge generated during the deintercalation process to the collector and to the external circuit. Meanwhile, the interaction between the electrode material and the collector interface determines the magnitude of the adhesion. If the adhesion is insufficient, firstly, it will not be able to play a self-supporting role; secondly, any impact on the battery may cause the electrodes to peel off, resulting in failure. The second interface is even more critical because it is the interface where most of the reactions take place and where the solid-liquid phase comes into contact. The electrolyte diffuses from the electrode surface to the interior under a concentration gradient. Once the active material is wetted by the electrolyte, there is a place for the reaction. The electrolyte helps transport lithium ions to this location from the other electrode.

2.5 Innovations in Electrode Design

In order to further optimize the reaction between the current collector and the active material interface and enhance the transmission of ions and electrons, Yuan et al. optimized the design of the current collector interface. Inspired by honeycombs, they etched honeycomb-like patterns on the current collector (see **Figure 10**). Through such a design, the contact area between the current collector and the active material can be effectively increased, which not only enhances adhesion but also significantly increases the charge transfer efficiency (Yuan *et al.*, 2019). On this basis, Kim et al. performed surface modification on the roller of the roller press to obtain an electrode layer with a surface pattern (Kim *et al.*, 2023). They also studied the type, size, and spacing of the patterns and stated that the sharp edges of polygonal patterns such as square and honeycomb would concentrate stress and damage the electrodes, while circular patterns would be more appropriate. The results of the experiments showed that electrodes with 250 μm circular patterns on the surface had the best capacity after 500 charge/discharge cycles at 1 C, and that all electrodes with patterns had better capacity retention and energy density than those without patterns. Liu et al. reported the vertical distribution of

the conductive agent has a significant effect on the performance of the battery. Electrodes with higher conductive agent content on the side closer to the current collector perform better, which is due to the fact that the lower-most layer of the electrode has more conductive agent content that can form more conductive pathways (Liu *et al.*, 2018).

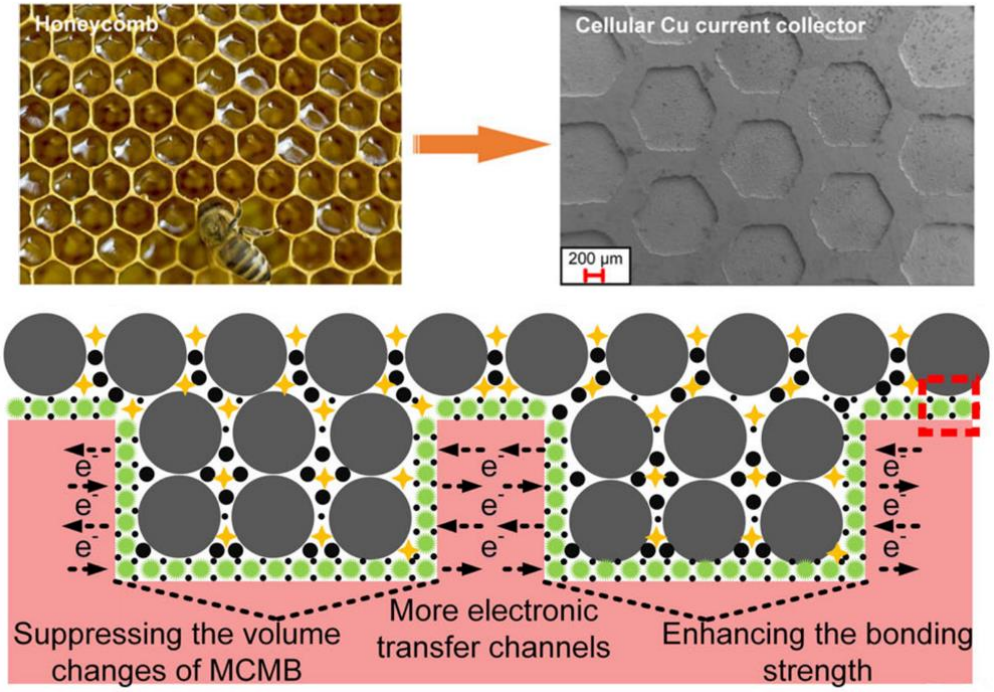

Figure 10: Current collector with honeycomb pattern on the surface (Yuan *et al.*, 2019).

Although thick electrodes (>200 μm) can provide more active materials and energy density, the reaction inside the thick electrode is incomplete due to poor lithium-ion transmission performance and high diffusion distance. On the side of the top of the electrode close to the electrolyte, the active material is completely infiltrated by the electrolyte, and the transmission distance of lithium ions is also very low, so the reaction can be complete. However, on the side of the bottom of the electrode close to the current collector, the active material is limited by the thick electrode, the electrolyte cannot be completely infiltrated, and the reactivity of the electrode is very low. This problem can be effectively solved by constructing a porosity gradient (Sukenik, Kasaei and Amatucci, 2023). The pores reduce the tortuosity and reduce the diffusion distance of lithium ions. Therefore, high porosity is constructed on the side close to the current collector, and the porosity is gradually reduced from bottom to top to form a gradient

(the top in contact with the electrolyte has the lowest porosity), which can effectively allow the electrolyte to penetrate to the bottom, and can also increase the diffusion capacity of lithium ions. An alternative concept is to construct ion channels to reduce the tortuosity so that the electrolyte and lithium ions can transmit further to the bottom. This idea can be accomplished by pores or conductive pathways that run straight from top to bottom. Mixing different cathode materials to achieve desirable properties is another common idea. Julien et al. studied the effect of the mixing ratio of olivine structure LFP to layered structure NMC on the electrode performance and indicated that NMC-LFP (70:30) blended electrode had the best discharge rate (Julien *et al.*, 2016). Constructing multilayer electrodes is also a favored approach, which is often applied in all-solid-state batteries, where they introduce buffer layers to reduce the problems of lithium dendrite puncture and electrode volume expansion (Wan *et al.*, 2023). Multilayer electrodes not only control the distribution of porosity and the distribution of binder, but also allow the design of protective layers to optimize the electrode surface. These four strategies are summarized in **Figure 11**.

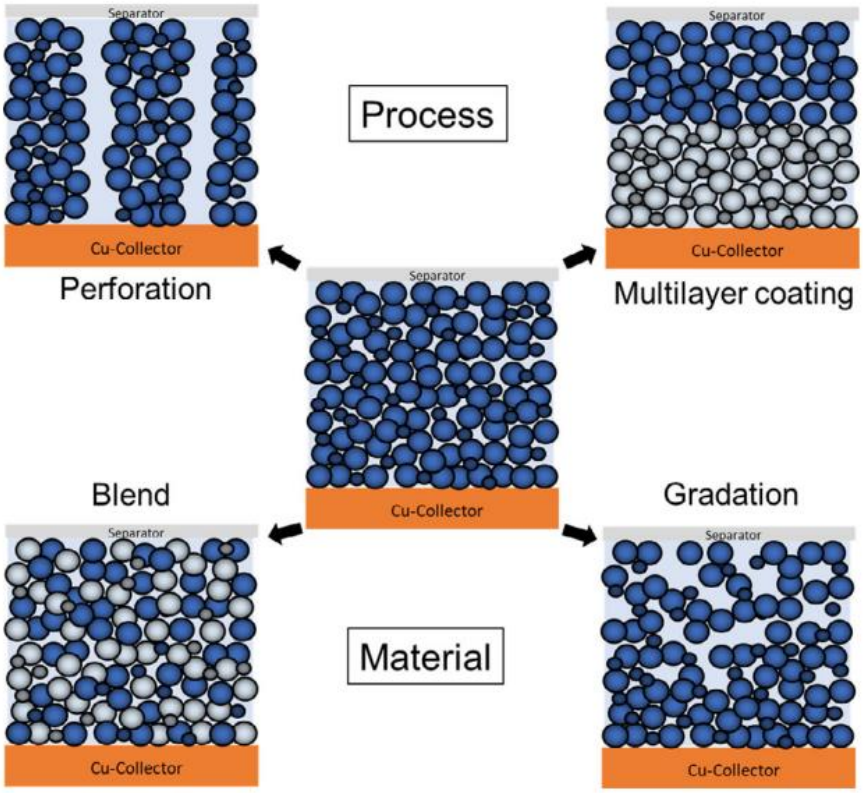

Figure 11: Four strategies of electrode design (Gottschalk *et al.*, 2022).

3 Methodology

3.1 Design of Coating Method

Although electrostatic spraying technology allows for very fine control of film thickness, its high cost and stringent environmental conditions, as well as the limited speed of electrode preparation, make this technology difficult to apply on a large scale. There is a need to find simpler and more efficient preparation methods that strike a perfect balance economically and technically. Though the direct pressing method (see **Figure 12 (a)**) is the simplest approach, this method can result in very dense material in some areas (generally near the pressing center or in areas with high material accumulation), due to the fact that the material is moving and dispersing from high to low under the pressure. It is also difficult to prepare electrodes with large area due to the poor mobility of solid particles. Meanwhile, excessive pressure risks crushing the active material particles. Another idea is similar to the doctor blade technique in wet coating, where a template is laid down on the current collector and a blade moves horizontally above the template and scrapes away the excess material from the top layer (see **Figure 12 (b)**). While this method can achieve thicknesses of a few microns in the wet coating, if it is applied to solid particles, once the height is very low, the solid particles in the bottom will slip along with the particles in the upper layer due to friction. This approach has been verified to work on heights greater than 2 mm (template height), but is difficult to realize on lower heights, such as 1 mm. More importantly, the final electrode thickness is often well below 2 mm.

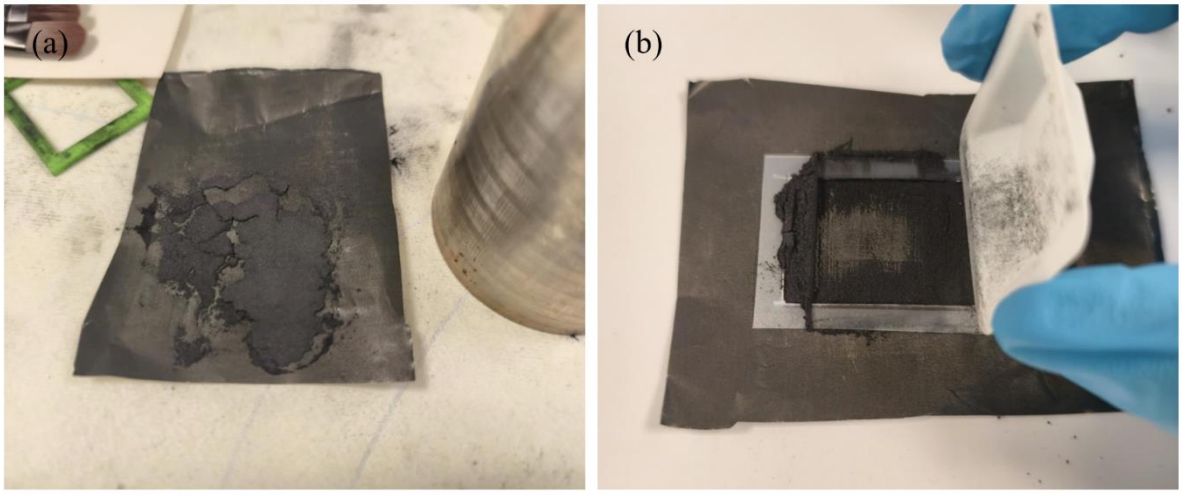

Figure 12: Coating methods: (a) Direct Pressing; (b) Moving Blade.

Based on this method (moving blade), inspired by plowing, a blade with a serrated shape was constructed, which can effectively solve the problem of particle sliding. This serrated blade allows solid particles to pass through the gaps, reducing friction and collisions between particles, thereby effectively spreading the particles evenly on the current collector. The width and height of the serrations are the most important parameters and influence the final result of the coating. As mentioned before, if the height is too low, it will still make the particles at the bottom get dragged by the particles at the top. If the width is too narrow, the particles will be blocked and cause collision and sliding. If the width is too wide, the uniformity of film formation will be affected. The height of the serration is similarly constrained. Excessive height can lead to noticeable peaks on the final surface, while insufficient height can impede the movement of particles. The thickness of the serrated tool is not critical, but it does need to be hard enough to resist wear and bending due to particle friction. The thickness of the final coating film is about 1 mm. This method is simple and efficient enough, and can be applied in large-scale industrial production. It should be noted that because the particle size and viscosity of electrode materials are different, the parameters of the serrations need to be adjusted case by case. Some materials, such as LFP, have a particle size of only 5 μm, but they tend to agglomerate, forming tens of microns agglomerated particles.

3.2 Electrode Design

LFP material has the advantages of low cost, high electrochemical stability, high thermal stability, and long cycle life. However, its relatively low specific capacity (170 mAh/g) hinders its path to the usage of high-end electric vehicles. Conversely, NMC811 material has the benefits of high ionic conductivity, high diffusion coefficient, and high capacity (200 mAh/g). Still, it has the drawbacks of high cost and poor stability on both long cycling and thermal properties. Their properties are shown in **Figure 13**. Therefore, an interesting strategy is to mix these two materials and explore whether both advantages of these two can be integrated or not. Another idea is to cover the NMC layer with LFP material, which has higher stability, as a protective layer (see **Figure 14**). As mentioned in **Chapter 2.4**, the top layer is in direct contact with the electrolyte and most of the reactions will take place there first, including the lithium-ion migration, redox reaction, and SEI/CEI formation. More importantly, the formation of lithium dendrites in lithium-ion batteries is a major factor contributing to battery failure. By introducing a passivated protective layer on the electrode surface, the deposition of lithium metal can be effectively reduced, the formation of lithium dendrites can be inhibited, and the cycle life of the battery can be greatly extended. However, it is worth pointing out that LFP is still acting as the active material for the electrode, not an ideal passivation layer in the conventional context.

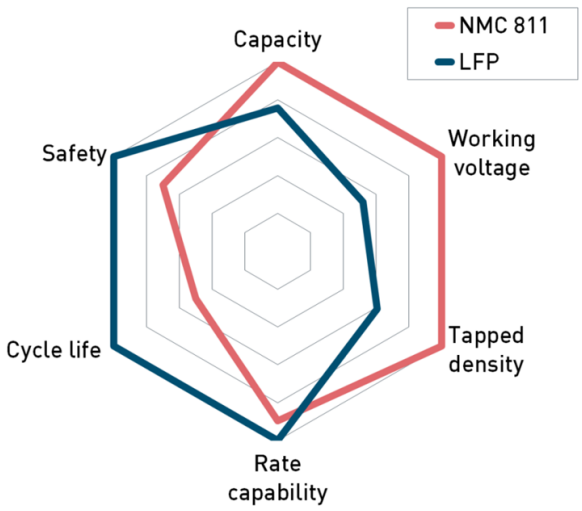

Figure 13: Spider chart of material properties of LFP and NMC811 (e-motec, 2022).

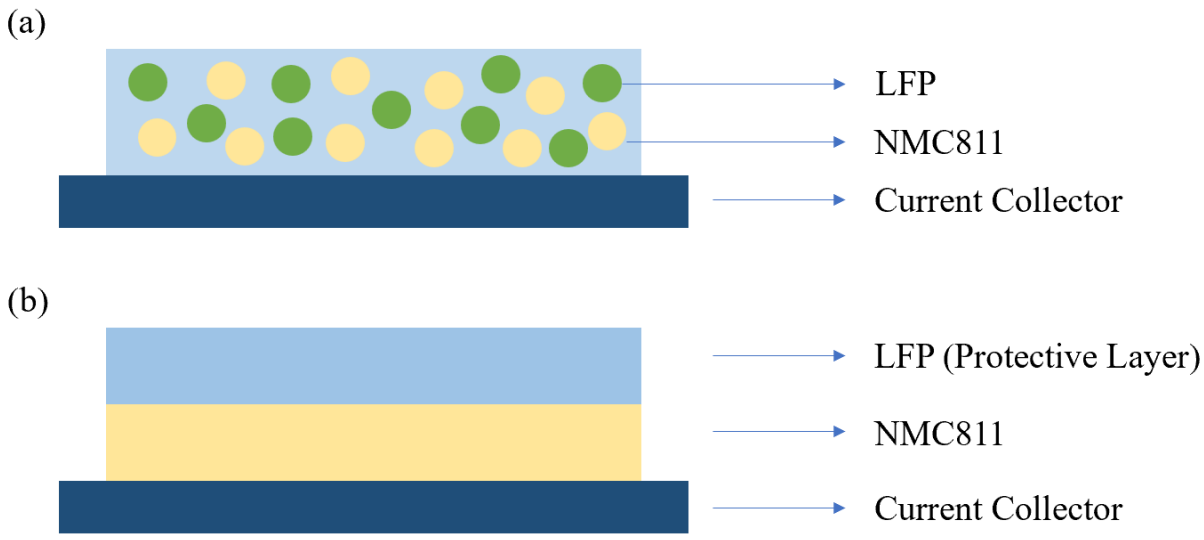

Figure 14: Configurations of two strategy electrodes: (a) LFP/NMC 1:1 wt% blended electrode; (b) NMC LFP double-layer electrode, with NMC811 as the first layer and LFP as the second layer. Here the ratio of electrode materials for each layer is 8:1:1 (active material: binder: conductive additive).

3.3 Fabrication Process of Electrode through Wet Coating Method

The active material (LFP or NMC811) was mixed with binder (PVDF) and conductive additive according to a ratio of 8:1:1, a total mass of 400 mg. A chemical spoon was used to manually grind and mix the materials for 5 minutes. A pipette was used to take 1 ml of NMP solution and transfer it to the mixed material. The obtained material was placed in a small glass flask on a magnetic stirrer and stirred using a magnetic stirring bar. Stirring was done at room temperature (25°C) at 300 RPM for 24 h. The coating process was carried out by a blade coating machine (see **Figure 15**), with the coating thickness set to 200 µm and the speed 4 mm/s. After coating, the samples were left in a fume hood for 24 h to dry and remove moisture. The dried samples were then sent to a vacuum oven and dried in a vacuum environment of 120°C for 24 hours to completely evaporate moisture and NMP solvent. The final electrodes are cut into 14 mm discs in a battery-punching machine. LFP: NMC811 1:1 (wt%) blended electrodes were also made through the above method.

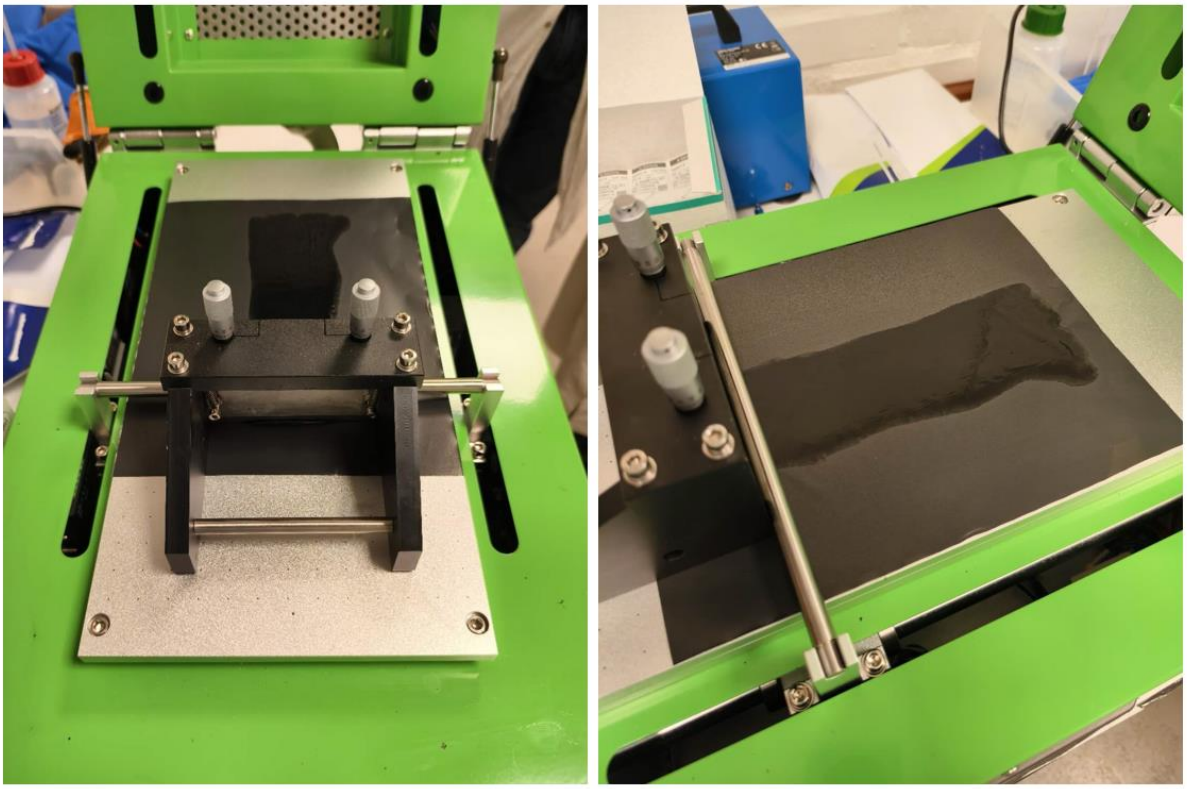

Figure 15: Blade coating machine for wet coating method.

3.4 Fabrication Process of Electrode through Dry Coating Method

The active material (LFP or NMC811) was mixed with binder (PVDF) and conductive additive according to a ratio of 8:1:1. The obtained material was placed in a reagent bottle on a magnetic stirrer and stirred using a magnetic stirring bar. Stirring was done at room temperature (25°C) at 400 RPM for 24 h, during which the mixing was done by manual shaking every 12 h. A serrated blade tool was used during the coating process to apply the mixed material onto the carbon coated aluminum foil (see **Figure 16**). The material was hot pressed using a roll-to-roll calendering machine (see **Figure 17**). The rotation speed of the roller was 4 mm/s. The final electrodes are cut into 14 mm discs in a battery-punching machine. LFP: NMC811 1:1 (wt%) blended electrodes were also made through the above method. For the double-layer electrode, the above steps are repeated based on the prepared first layer to prepare the second layer of electrodes.

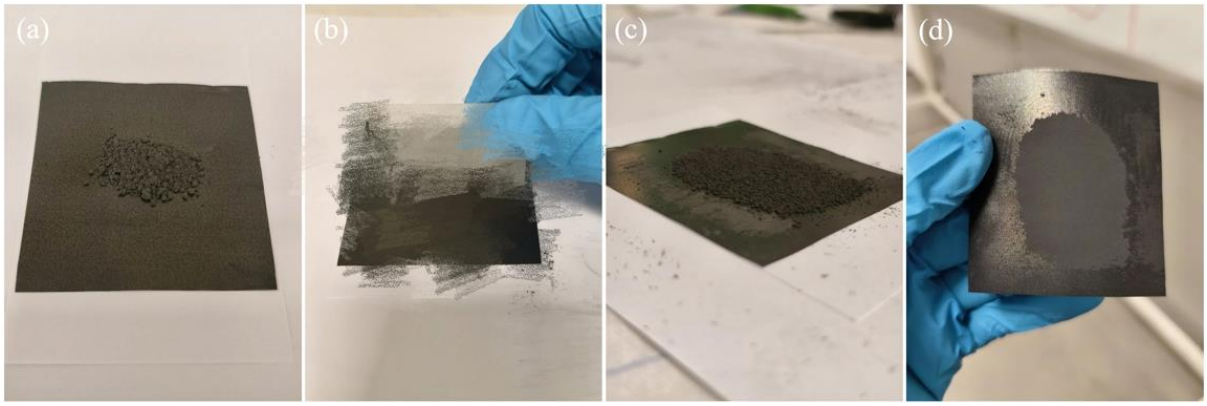

Figure 16: Illustration of the dry coating process, from left to right: (a) stacking of feedstock; (b) spreading of feedstock using a serrated blade tool to form a uniform film; (c) appearance of the electrode film before sending to the calendering machine; (d) final appearance of the electrode after hot pressing. Here the active material is LFP.

Figure 17: Roll-to-roll calendering machine for dry coating method.

3.5 Battery Assembly

The fabricated electrodes (cathodes) were assembled into half cells in a glove box (in a condition of inert gas, where H_2O < 1 ppm, O_2 < 1 ppm). The assembly sequence is as shown in **Figure 18**, proceeding from the bottom up. Li sheets were used as counter electrodes (anodes). Celgard 2325 was used as the separator. And the electrolyte was 1.0 M $LiPF_6$ in a volumetric ratio of EC/DMC=50/50 (Lithium Hexafluorophosphate, $LiPF_6$; Ethylene Carbonate, EC; Dimethyl Carbonate, DMC). For the wet coating method, 2-3 drops of electrolyte were added to the cathode and anode surfaces respectively. For the dry coating method, an excess amount of electrolyte (10 drops) was dripped from the side gap to the inside before the final pressing to prevent the dry electrode from bending due to contact with the electrolyte and affecting assembly. Finally, the assembled batteries were pressed and fixed.

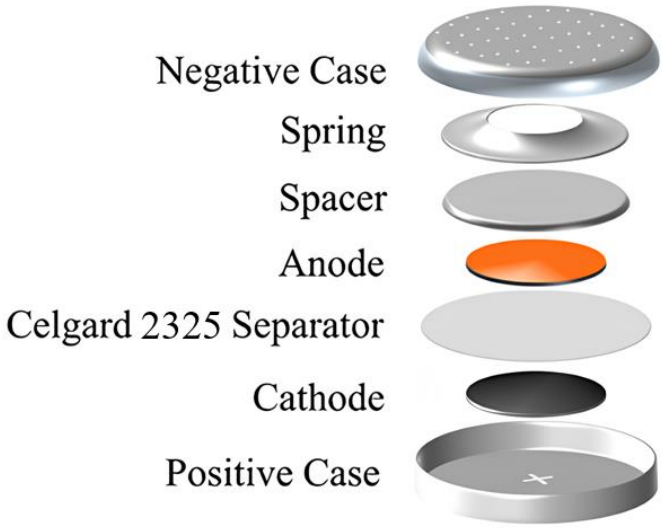

Figure 18: Assembly structure of the coin cell (Xue *et al.*, 2023).

3.6 Characterization of Battery Performance

Before starting this section, it's important to clarify the mass of active materials because it will determine the specific capacity and will be filled in the test system. The total mass of a single-layer electrode by the wet coating method is generally 6-7 mg, while the total mass of a single-layer electrode by the dry coating method is generally 20 mg. And the total mass of the double-layer electrode prepared by dry coating technology is usually around 30 mg. The total mass here includes the mass of the carbon-coated aluminum foil (current collector), 4.42 mg, and the mass of the remaining electrode materials. Therefore, the mass of the electrode active material is the total weight minus the mass of the carbon-coated aluminum foil, multiplied by the ratio of the active material to the electrode material. Ultimately, for the wet coating technique, the mass of active material typically ranges from 1-2 mg for single-layer electrodes. In contrast, for dry coating technology, the active material mass of a single-layer electrode generally ranges from 10 to 15 mg, and for a double-layer electrode, it ranges from 20 to 30 mg.

Cycling and Rate Capability Test

The prepared coin cells were tested in the LAND battery test system. The battery was first left to stand for 6 hours to allow the electrolyte to fully infiltrate the electrodes. Then, the charge and discharge tests were performed with a voltage range of 2.5 V to 4.2 V. For the single-layer electrode, the two cycles were performed at a C-rate of 0.1C for activation. C rate means how long it would take to charge or discharge a battery, 1 C means it will be charged or discharged in one hour and 2 C means it will finish charge or discharge in a half hour. For the double-layer electrode, the first two cycles were performed at a C-rate of 0.05C for activation (because its current density is equivalent to 0.1C for a single-layer electrode). The specific capacity of LFP was set to 160 mAh/g for testing (Lung-Hao Hu *et al.*, 2013). And the specific capacity of NMC811 was set to 180 mAh/g (Vidal Laveda *et al.*, 2019). The specific capacity of LFP: NMC811 1:1 (wt%) blended electrode was set to 170 mAh/g. It is worth mentioning that because the actual capacity needs to be tested, the value filled in here is the test value of charging and discharging based on the theoretical value of the program. Then some coin cells were tested for 200 cycles in 0.2C from 2.5V to 4.2V for the cycling test and some coin cells were tested in 0.1C-0.2C-0.5C-0.1C every five cycles for the rate capability test.

Cyclic Voltammetry (CV)

Cyclic Voltammetry (CV) test was performed in EC- lab battery test system. The battery was left for 6 hours and then scanned at a rate of 0.1 mV/s from the starting voltage of 2.5 V to the terminal voltage of 4.2 V, and then scanned from 4.2 V back to 2.5 V for one cycle, with a total of 5 tests, and the best cycle was taken as the result.

4 Results

4.1 Coating Result

The coating result has a significant influence on the electrode performance. **Figure 19** shows what these electrodes look like after wet/dry coating method. The wet coating process has a smoother surface, while dry coating produces visible holes on the surface of the electrode. The electrodes of the dry coating process have a load (mass) three times that of the electrodes of the wet coating process. The LFP electrode exhibits a light gray color, the NMC811 electrode exhibits a darker black color, and the blended electrode looks closer to the LFP.

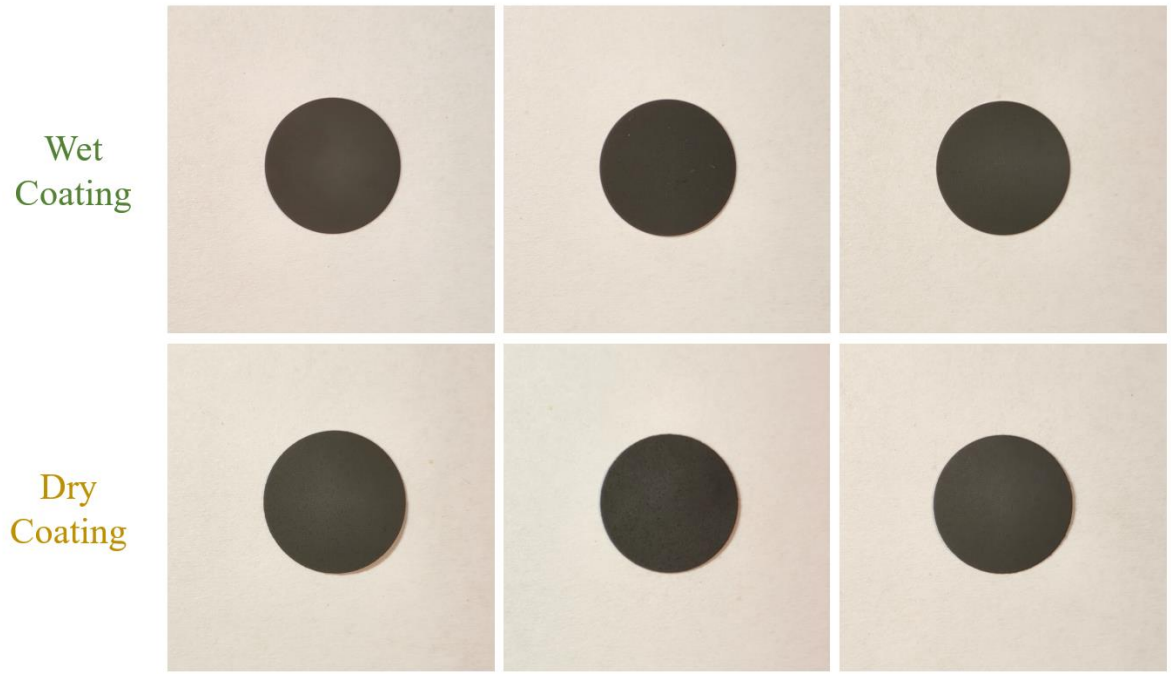

Figure 19: Final appearance of electrodes through the wet coating and dry coating, from left to right: LFP, NMC811, LFP/NMC 1:1 blended, single-layer.

4.2 Morphology of Electrodes

In order to observe the morphological properties of the electrodes even further, scanning electron microscopy (SEM) was used by JEOL JSM-7800F Prime.

LFP Electrode

Figure 20 shows the morphology of the LFP electrode. It can be seen that the electrode surface of the wet coating process is very flat, while the electrode of the dry coating process has a rougher surface and shallow indentations. The right image shows the distribution of electrode materials after zooming in. The particle size of LFP active material ranges from 500 nm to 1 μm, with a crystal appearance. The black soft layered conductive additive is distributed between the LFP active materials, which plays a role in enhancing the conductivity and boosting electron transportation. PVDF powder has the smallest particle size, approximately 100-200 nm. It is precisely because of its small size that it can be dispersed more freely on the surface of various materials, playing a role in connecting and binding.

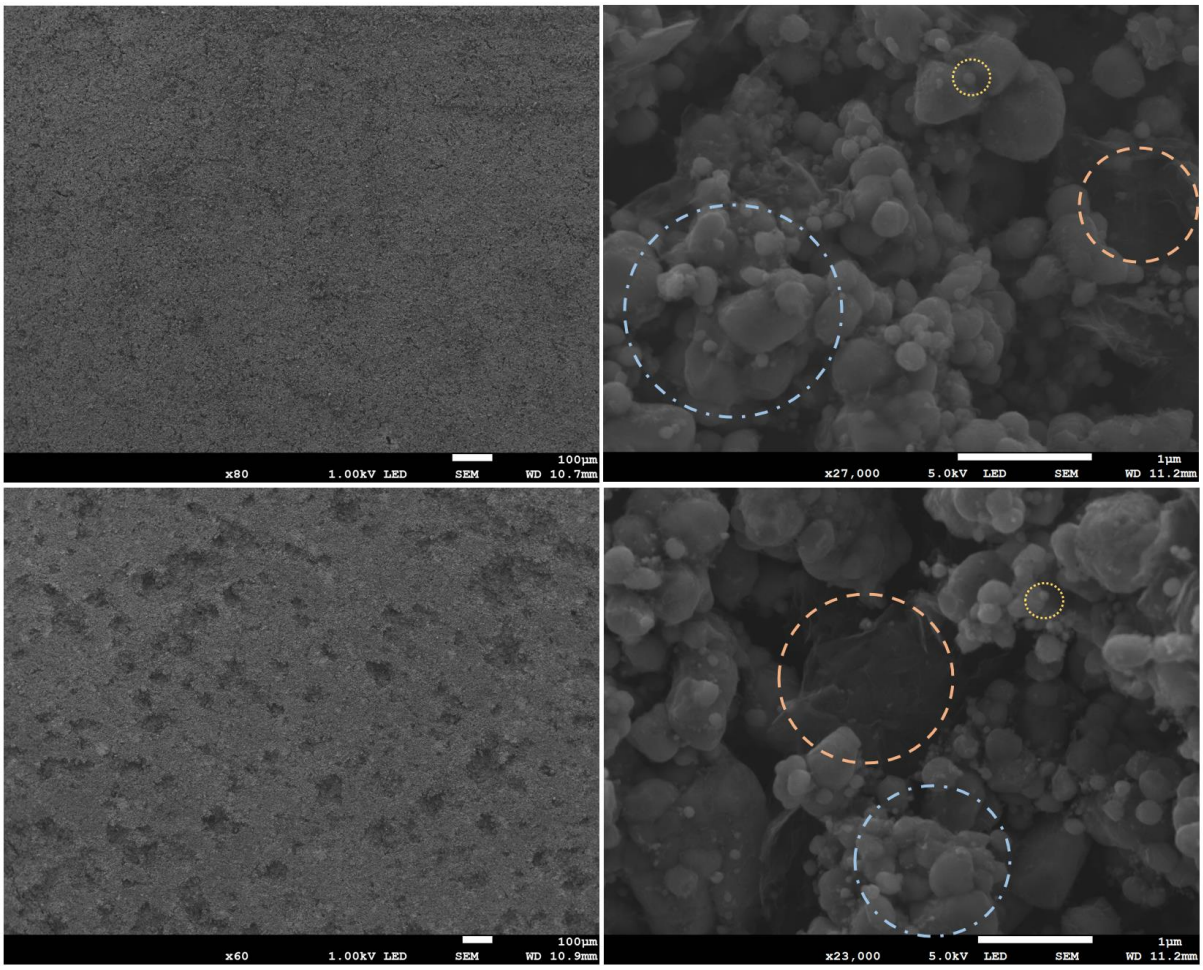

Figure 20: Morphology of LFP electrode, First Row: Wet Coating; Second Row: Dry Coating; the blue dashed circle shows LFP particles; the orange dashed circle shows conductive additive; and the yellow dashed circle shows PVDF binder.

NMC811 Electrode

Figure 21 shows the appearance of the electrode with NMC811 as the active material. Likewise, the wet coating method presents a more intact surface than the dry coating method. The NMC811 material has a larger particle size (around 10 μm) compared to the LFP particles and exhibits a spherical shape. This spherical appearance is more conducive to observing the changing of the material before and after the reaction, but it also makes it more susceptible to the risk of particle breakage due to the pressure. For the wet coating process, PVDF may be difficult to see due to the small distribution of the selected area. For the dry coating process, PVDF has been hot-melted at 200℃, so the particles are not visible but adhere to the surface of other materials. Here, the layered structure of conductive additive is better presented.

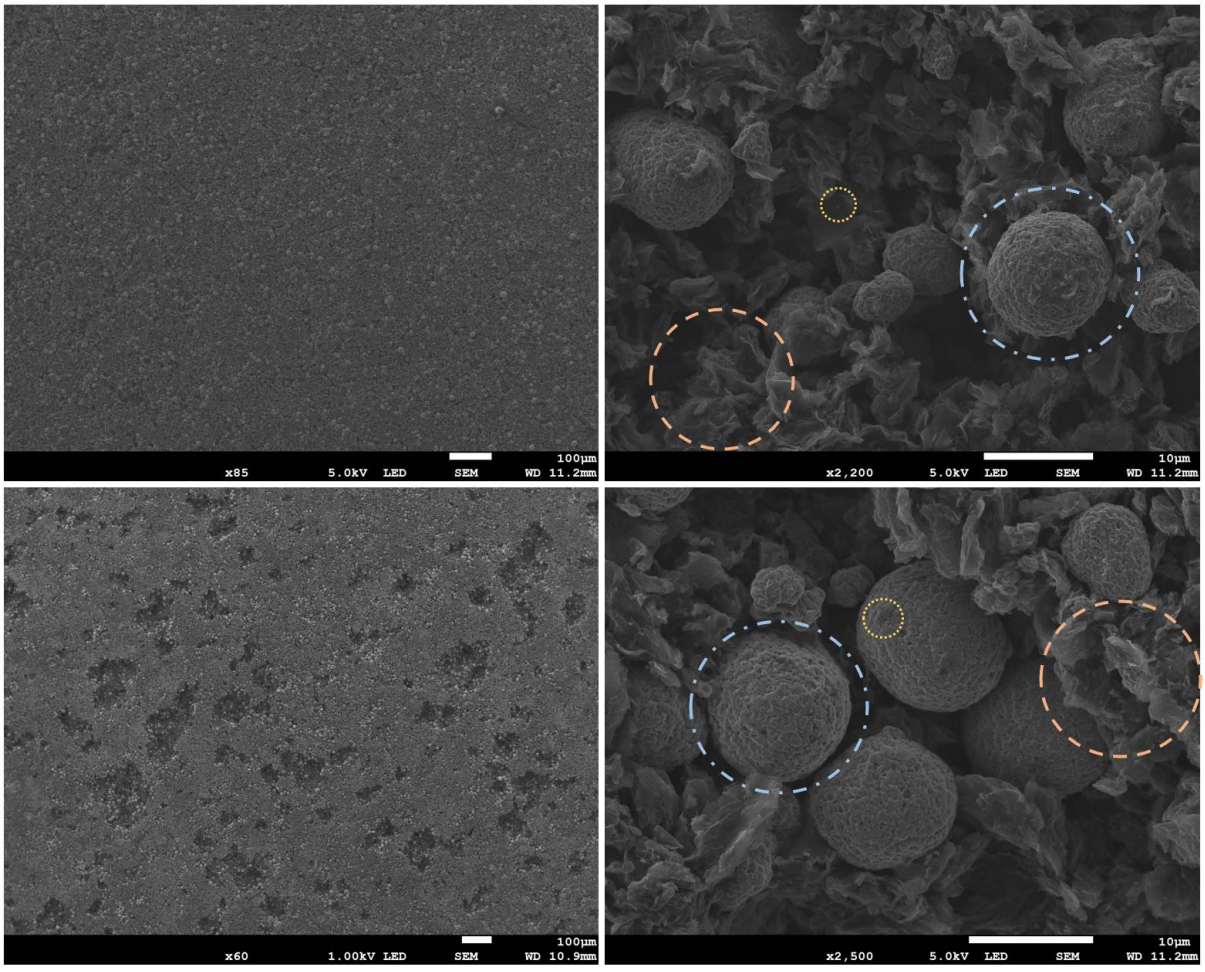

Figure 21: Morphology of NMC811 electrode, First Row: Wet Coating; Second Row: Dry Coating; the blue dashed circle shows NMC811 particles; the orange dashed circle shows conductive additive; and the yellow dashed circle shows PVDF binder.

LFP/NMC 1:1 Blended Electrode

Interesting results are presented in **Figure 22** for the LFP/NMC 1:1 blended electrode. In contrast, the dry coating LFP/NMC 1:1 blended electrode has a smoother surface than the wet coating electrode sample. By magnifying the surface, it can be observed that the NMC particles, due to their larger particle size, squeeze the adjacent interface, which leads to the initiation and propagation of cracks. This type of crack is not uncommon in wet processes because it is a side effect of the evaporation of solvent and moisture. It occurs but is just not obvious in the previous samples of single active material. As the crack prolongs, the electrode is at risk of fracture and eventual failure.

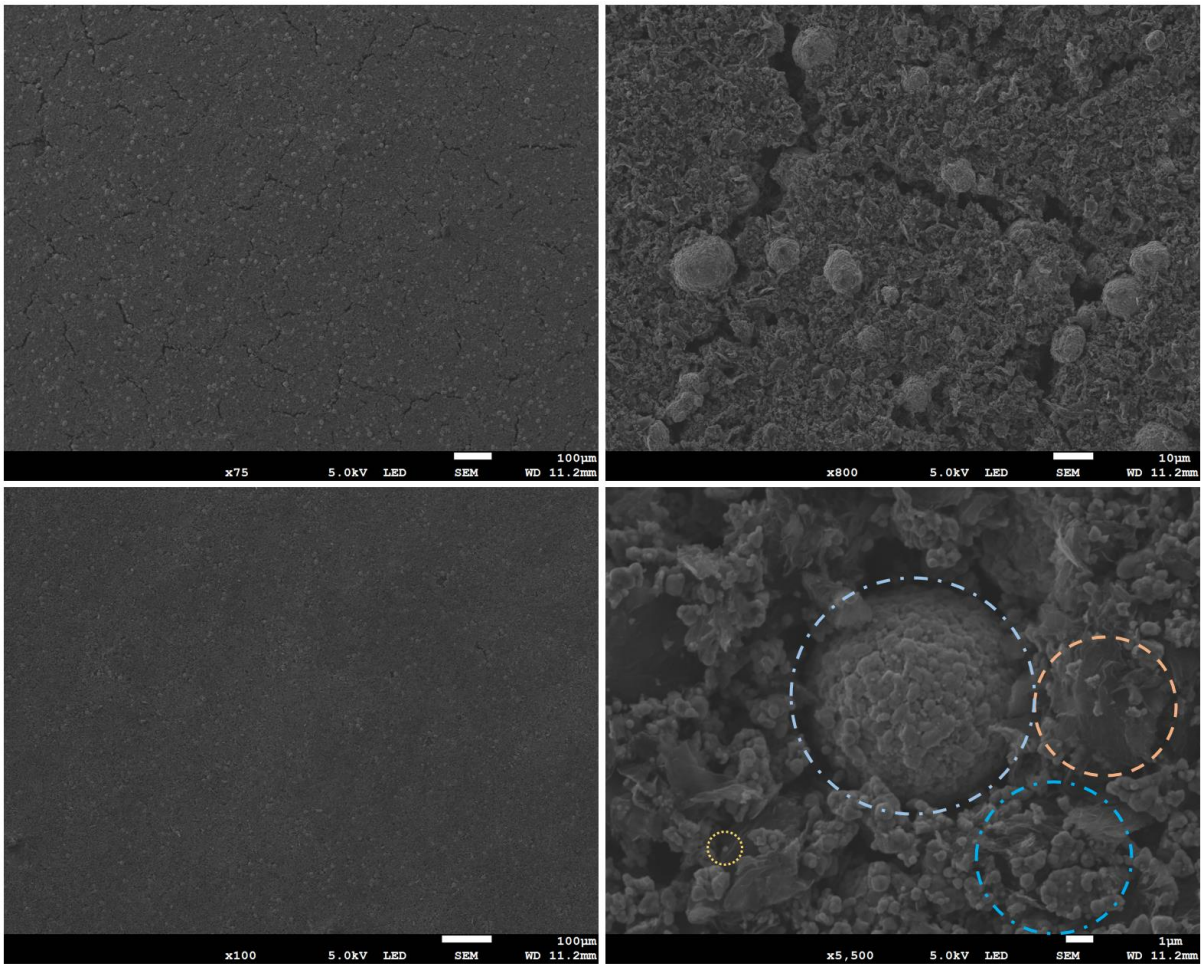

Figure 22: Morphology of LFP/NMC blended electrode, First Row: Wet Coating; Second Row: Dry Coating; the light blue dashed circle shows NMC811 particle; the deep blue dashed circle shows LFP particles; the orange dashed circle shows conductive additive; and the yellow dashed circle shows PVDF binder.

Cross Section

It is necessary to study the cross section of the electrode because it can provide much important information such as thickness, density, porosity, tortuosity, particle integrity, material distribution and so on. **Figure 23** illustrates the cross section of several electrodes. For the same single-layer electrodes, the electrode thickness of the wet coating technique is the smallest, only 40 μm. In comparison, the electrode thickness of the dry coating technique is around 110 μm (without regard to the current collector). The thickness of the double-layer electrode is well controlled to be about twice that of the single layer, around 240 μm. In **Figure 23 (c)**, the stratification phenomenon can be clearly observed, and the thickness of the LFP layer is very close to that of NMC811, which is approximately 120 μm, indicating that the preparation parameters are in line with expectations (to keep the thickness of each layer equal). In all of the figures, NMC811 shows a complete particle morphology, indicating that this pressure does not result in particle fragmentation of NMC811. The NMC811 single-layer electrode prepared by dry coating still retains a certain amount of porosity, which is sufficient for the electrolyte to penetrate to the bottom. Electrodes containing LFP materials are less porous and denser because LFP has a smaller particle size.

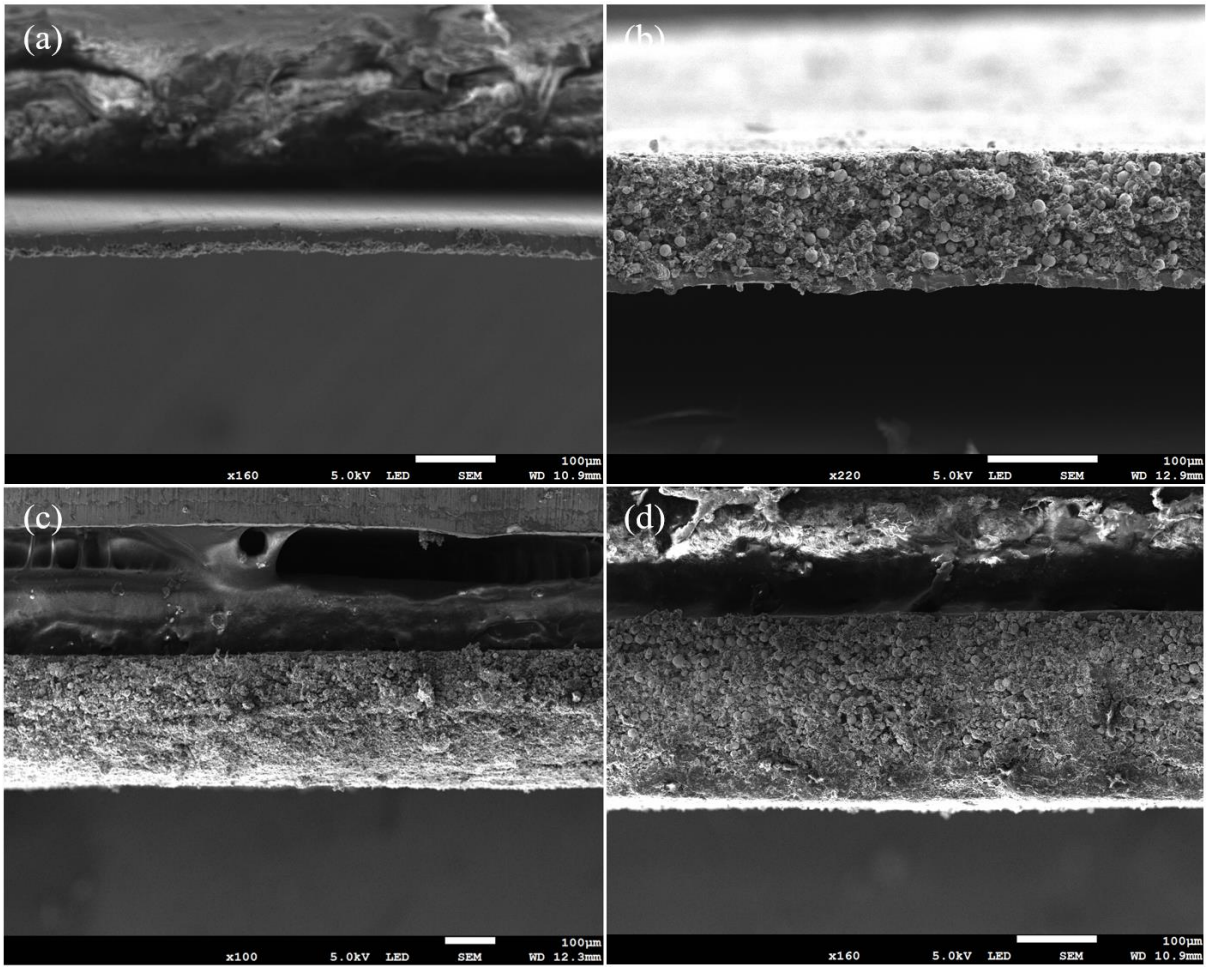

Figure 23: Cross section of different electrodes: (a) single-layer NMC811 electrode by wet coating; (b) single-layer NMC811 electrode by dry coating; (c) dry coating double-layer electrode with the first layer NMC811 and the second layer LFP; (d) dry coating double-layer NMC811 electrode. Note: except for (b), others are reverse which means the current collector is at the top and the layer close to the top is the first layer. Image (d) is only used as a reference for the thickness of the double-layer electrode and is not the focus of this study.

4.3 Electrochemical Performance

4.3.1 Cycling Test

LFP Electrode

LFP material has a good fame for its excellent stability, which can be seen from the test results (see **Figure 24**). The LFP electrodes prepared by both methods exhibited good Coulombic efficiency and small capacity decay. For the wet coating LFP electrode, it has an initial Coulombic efficiency of 98.26% and a capacity value of 146.1 mAh/g. It maintains an efficiency of 93.66% and a capacity of 138.6 mAh/g after 100 cycles, with a capacity retention rate of 94.9%. The LFP electrode prepared by the dry coating shows even better performance. Its Coulombic efficiency is maintained at around 99%, and it shows a higher initial capacity of 156.2 mAh/g. After 48 cycles, its efficiency slightly drops to 96.27% and the capacity value declines to 154.8 mAh/g, with a capacity retention rate of 99.1%. Similarly, after 48 cycles, the capacity of the wet coating LFP electrode is only 142.9 mAh/g, and the retention rate is only 97.8%. Whether in terms of initial capacity, capacity retention rate, or Coulombic efficiency, the dry coating LFP electrode shows better performance. However, the reason for this distinction may not lie in the fabrication method, but rather in the individual performance differences of the batteries. More data is needed to verify this.

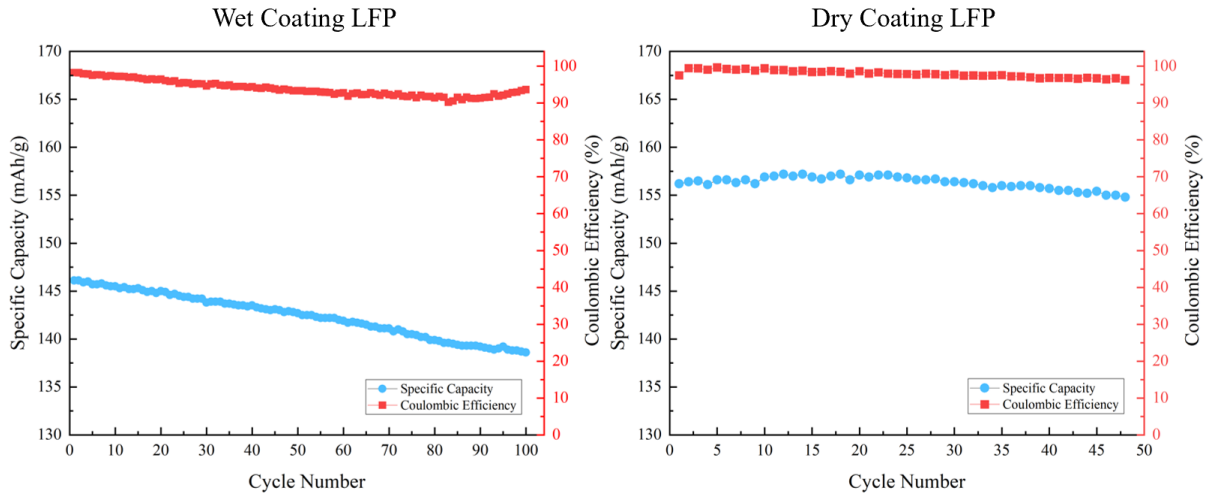

Figure 24: Cycling test for LFP single-layer electrodes at 0.2C:

(a) Wet coating; (b) Dry coating.

NMC Electrode

The NMC811 has a higher capacity value than the LFP material, which is shown in **Figure 25**. The performance of wet coating NMC electrodes varies considerably due to the low stability of the NMC811 material as well as its sensitivity to the preparation process. In order to obtain a standard performance of NMC wet coating electrodes, four groups of NMC811 wet coating samples were prepared, with a total of dozens of NMC811 electrodes. The sample here is after selection and provides a relatively reasonable result. The wet coating NMC electrode demonstrated an initial capacity of 163 mAh/g and decreased to 143.5 mAh/g after 85 cycles with 88% capacity retention rate. And for the dry coating NMC electrode, it has a higher specific capacity value of 181.8 mAh/g compared to the wet coating method. And its Coulomb efficiency is 99.25% at the first cycle. But after the 34th and 45th cycle, it began to experience a more noticeable decline in both efficiency and capacity. After the final 57 cycles, its capacity decayed to 172.1 mAh/g with a Coulomb efficiency of 94.17%, with a capacity retention rate of 94.7%. For a fair comparison, the specific capacity after 57 cycles for wet coating NMC electrode is 153.9 mAh/g and the capacity retention rate is 94.4%. It can be seen that the two NMC electrodes exhibit very similar capacity degradation performance despite the initial capacity difference. It is also proved that the capacity decay in long cycling of NMC material is more pronounced than that of LFP material.

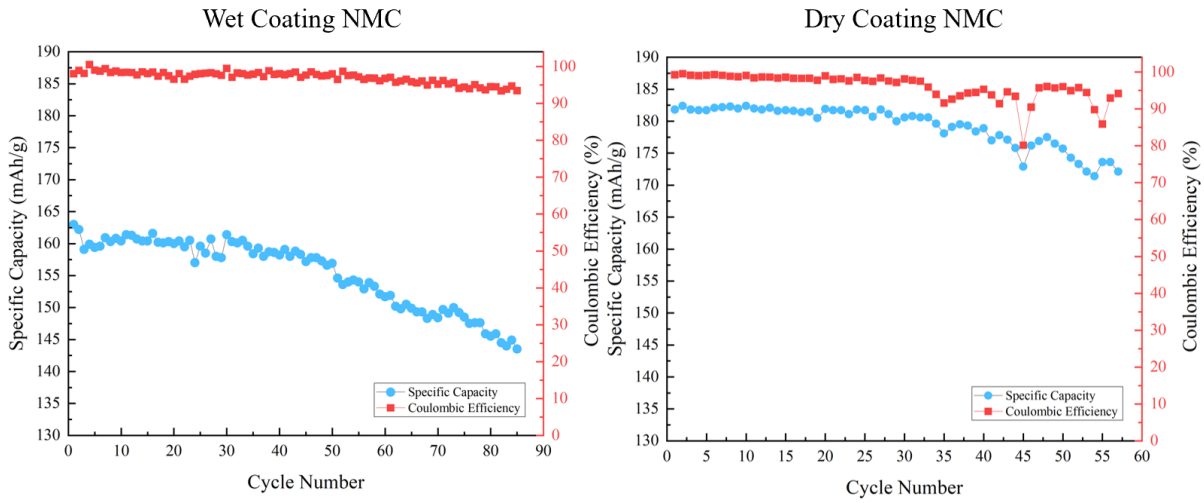

Figure 25: Cycling test for NMC single-layer electrodes at 0.2C:

(a) Wet coating; (b) Dry coating.

LFP/NMC Blended Electrode

As shown in **Figure 26**, The cycling performance of the blended electrodes is not as good as expected. For the wet coating electrode, its capacity gradually increases with the progress of cycles, which is completely a different pattern from other electrodes. And surprisingly, even though its Coulomb efficiency did not fluctuate much in the early stage, the capacity value leaped. Its initial capacity is only 130.1 mAh/g, but it rose to 141.6 mAh/g after the 26th cycle and gigantically spike to 159.2 mAh/g at 40th cycle. It is speculated that most of the NMC material began to discharge at this time. After the last 45th cycles, its capacity value reached 166.7 mAh/g, which is much higher than the initial value. It is worth noting that although its capacity skyrocketed in the 40th cycle, its Coulombic efficiency also dropped greatly. At this time, the battery can be considered as failure and has no meaning. The dry coating blended electrode showed an initial capacity of 173.3 mAh/g, and maintained a value of 165.1 mAh/g after 78 cycles. Nevertheless, its Coulombic efficiency dropped intermittently throughout the period and significantly declined at 45th, 55th cycle, indicating a poor stability. Although the performance of both is not satisfactory, the dry coating blended electrode still performs better than the wet coating blended electrode, because it has higher capacity most of the time and degrades later. But it also means that direct blending is not a good strategy.

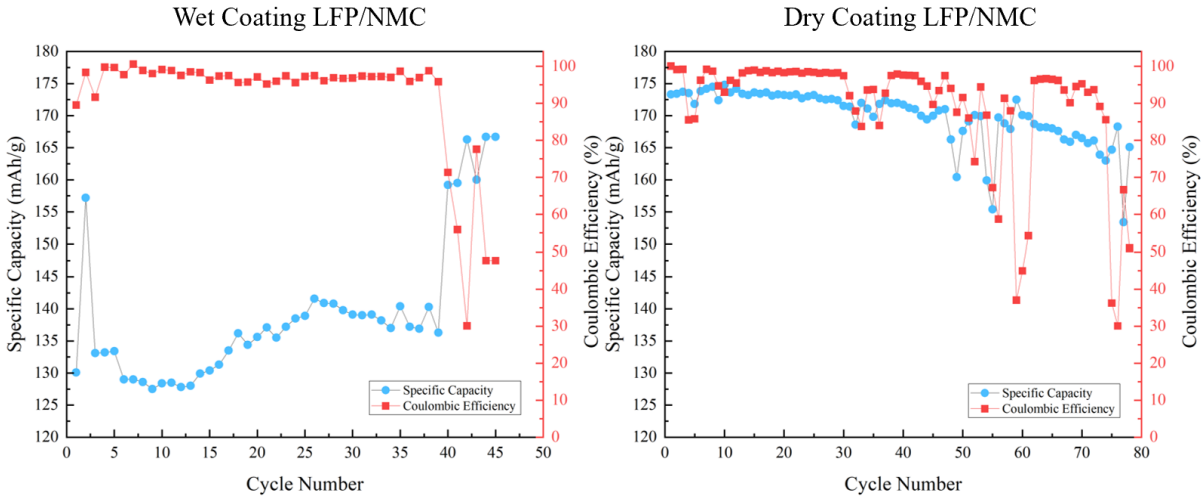

Figure 26: Cycling test for LFP/NMC blended single-layer electrode at 0.2C:

(a) Wet coating; (b) Dry coating.

NMC LFP Double-Layer Electrode

The NMC LFP double-layer electrode showed better stability compared to the single-layer directly blending electrode (see **Figure 27**). It not only has an initial capacity of 174.8 mAh/g, but also maintains a Coulombic efficiency of more than 90% in the first 40 cycles. A significant efficiency decay occurred in the 43rd cycle, and the efficiency was only 58.14% in the 45th cycle. Interestingly it showed excellent stability in the vast majority of cycles, but like all blended electrodes, their failure occurred near the 40th cycle. The deep mechanism can be further developed in future studies.

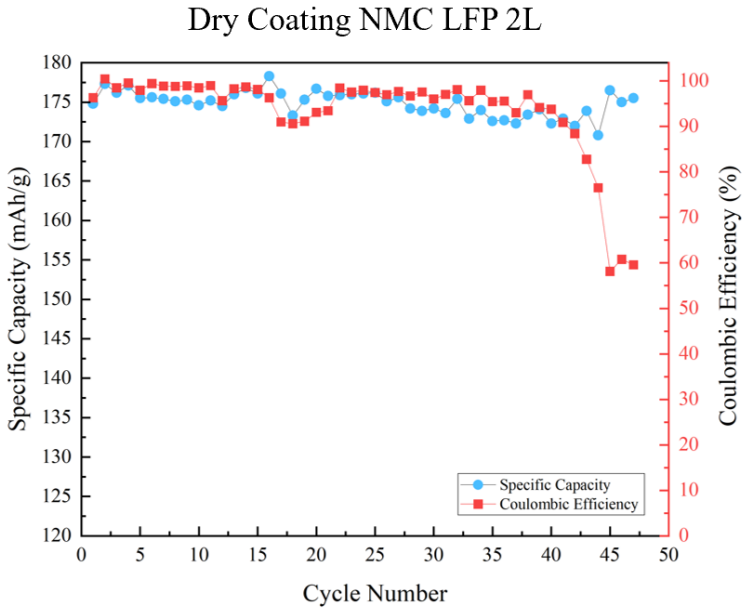

Figure 27: Cycling test for NMC LFP double-layer electrode at 0.2C.

4.3.2 Rate Capability Test

LFP Electrode

The LFP electrodes prepared by the two methods have highly similar rate performance (see **Figure 28**). At 0.1C, they all show a value close to the theoretical 160 mAh/g, which is 159 mAh/g. At 0.2C, their values drop slightly to 157 mAh/g. They maintain a good value of 150 mAh/g even at 0.5C.

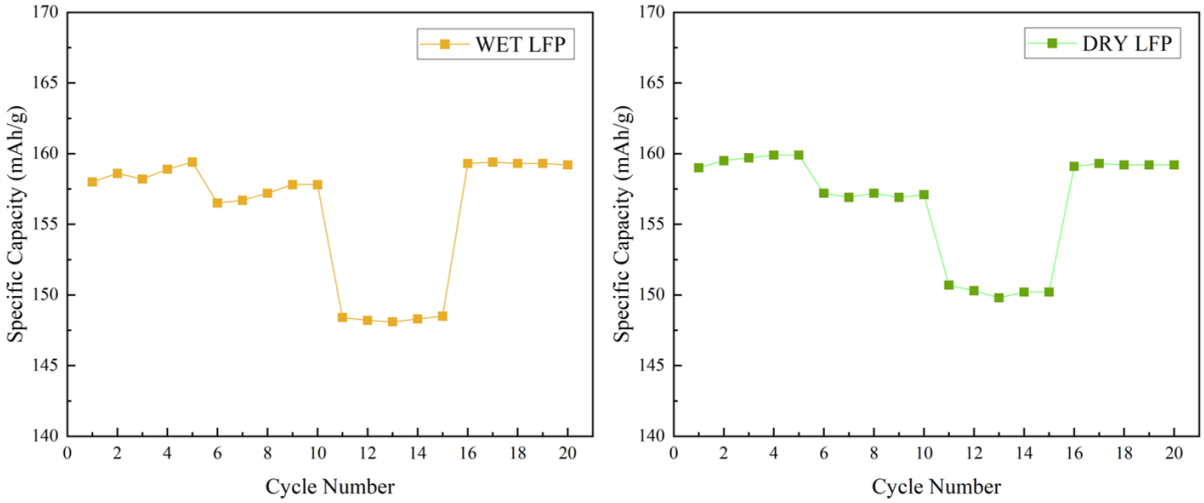

Figure 28: Rate capability test for LFP single-layer electrodes, tested at 0.1C-0.2C-0.5C-0.1C within a voltage range from 2.5 V to 4.2 V.

NMC Electrode

As mentioned earlier, the NMC811 material is very sensitive to the preparation process, and therefore the data measured for different sample sets are highly variable. The poorer performance of wet coating NMC811 electrode was selected for **Figure 29**, while a very good result of wet coating NMC811 was presented in **Figure 30**. It can be seen that the performance of the poorer group at each rate is even worse than that of LFP, and a very low capacity value was obtained at 0.5C. However, the better group showed an extremely excellent rate performance, achieving a capacity of nearly 195 mAh/g at 0.1C, which is very close to the theoretical capacity of NMC811 in the voltage range of 2.5 V - 4.2 V. And even at 0.5C, it can maintain a specific capacity of up to 176 mAh/g. Its high rate performance is not inferior to

that of LFP material. The NMC electrode prepared by the dry coating, on the other hand, has a more consistent performance performance and its rate performance is in between the two wet samples. But its capacity decayed remarkably at 0.5C.

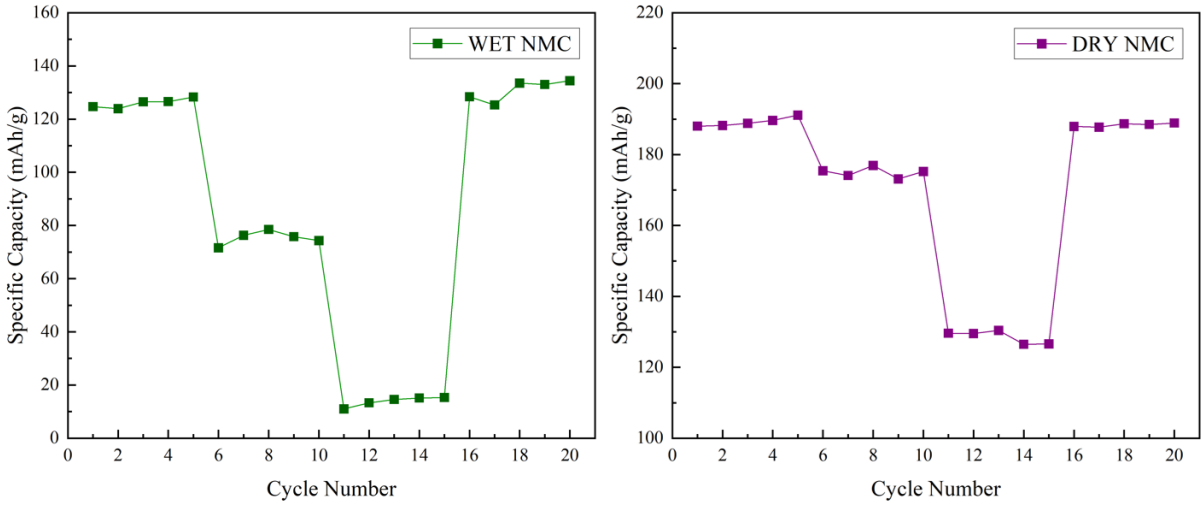

Figure 29: Rate capability test for NMC single-layer electrodes, tested at 0.1C-0.2C-0.5C-0.1C within a voltage range from 2.5 V to 4.2 V.

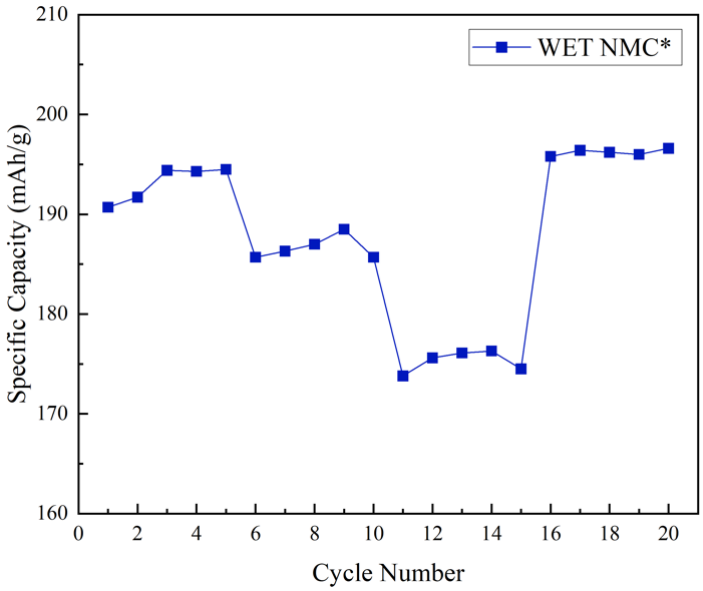

Figure 30: Rate capability test for another group NMC wet coating electrode, tested at 0.1C-0.2C-0.5C-0.1C within a voltage range from 2.5 V to 4.2 V.

LFP/NMC Blended Electrode

For LFP/NMC blended electrodes, a huge difference occurs. The blended electrode through wet coating has much lower capacity in all rate tests (as shown in **Figure 31**). The wet coating electrode shows an initial specific capacity of 115 mAh/g at 0.1C, 109 mAh/g at 0.2C, and 75 mAh/g at 0.5C. However it shows an increasing capacity for the last 0.1C test, which means in the previous test, the material was not fully utilized. This situation also occurred in several other groups of sample tests, indicating that the LFP/NMC blended electrode prepared by the wet coating method has the characteristics of incomplete reaction. The reason for this phenomenon is presumably because the activity of NMC particles is inhibited by the action of LFP and solution, so the capacity is very low in the first few cycles. On the contrary, the electrode prepared by dry coating has very high capacity and low capacity decay at high C-rate. At 0.1C, the dry coating electrode shows a capacity of 182 mAh/g. The capacity of the dry coating electrode is 175 mAh/g at 0.2C, and 162 mAh/g at 0.5C, respectively. All electrodes exhibited a higher capacity than the initial value at the last 0.1C. It can also be found that the dry coating blended electrode shows an increasing trend in each rate test. This phenomenon is similar to that of the wet coating blended electrode and is produced by the thorough activation of NMC particles after cycling. The result shows the blended electrode prepared by the dry coating method has excellent rate performance.

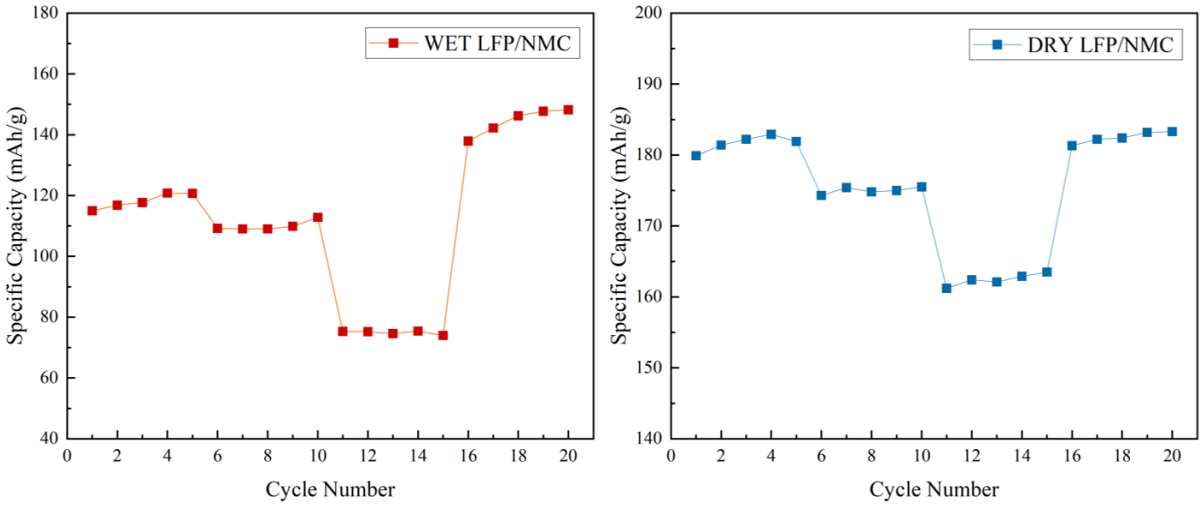

Figure 31: Rate capability test for LFP/NMC blended single-layer electrodes, tested at 0.1C-0.2C-0.5C-0.1C within a voltage range from 2.5 V to 4.2 V.

NMC LFP Double-Layer Electrode

The rate performance of the NMC LFP double-layer electrode is not much different from that of the single-layer electrode (as shown in **Figure 32**). It has an average capacity of 183 mAh/g at 0.1C and 174.8 mAh/g and 158.4 mAh/g at 0.2C, 0.5C respectively.

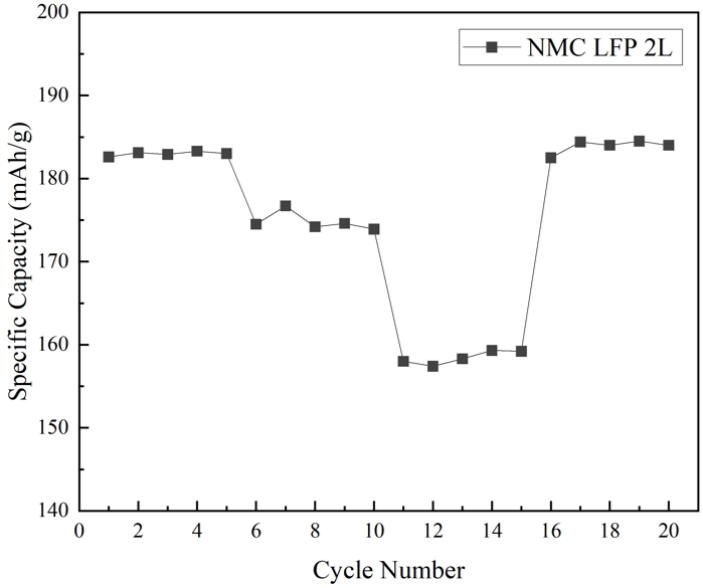

Figure 32: Rate capability test for NMC LFP double-layer electrode, tested at 0.1C-0.2C-0.5C-0.1C within a voltage range from 2.5 V to 4.2 V.

4.3.3 Cyclic Voltammetry (CV)

Cyclic voltammetry is a practical electrochemical analysis technique that studies the kinetics and mechanism of electrochemical reactions by applying a linearly varying potential to the electrode surface and probing the corresponding current change. The resulting image can reveal redox peak potentials, peak currents, and the reversibility of the reaction (Elgrishi *et al.*, 2018).

LFP Electrode

The first peak generated during the forward scan (scanning from low to high voltage) is the oxidation peak. In electrochemistry, the faradaic current is the current generated by the redox reaction. For the wet coating LFP electrode, as the applied voltage (contributing to non-Faraday

current) gradually increased, at 3.46 V, the electrode surface began to react and the Faraday current began to increase (see **Figure 33**). The LFP electrode prepared by the wet coating method reaches a peak value at 3.60 V, and the corresponding oxidation peak current is 1.02 mA while that of the dry coating occurs at 3.67 V and the corresponding oxidation peak current is 3.53 mA. The reverse scan (voltage from high to low) yields the reduction peak. The reduction peak for the wet coating method occurs at 3.29 V, corresponding to a peak current of - 0.76 mA. The reduction peak for the dry coating appears at 3.24 V with a peak current of - 2.52 mA. It can be clearly seen that the electrode prepared by dry coating has a larger peak current, which is due to the fact that it has more active material. Polarization contributes to the voltage gap between the oxidation peak and the reduction peak. The wet coating has a smaller voltage difference of 0.31 V compared to 0.43 V for dry coating technology, which means a better result. However, since the number of selected CV cycles is different, and as the cycle numbers increase, a tendency of a smaller gap for dry coating LFP is shown, thus it cannot be fully proved that the wet coating LFP electrode has a smaller polarization. Both curves show high a degree of symmetry, indicating excellent chemical reversibility.

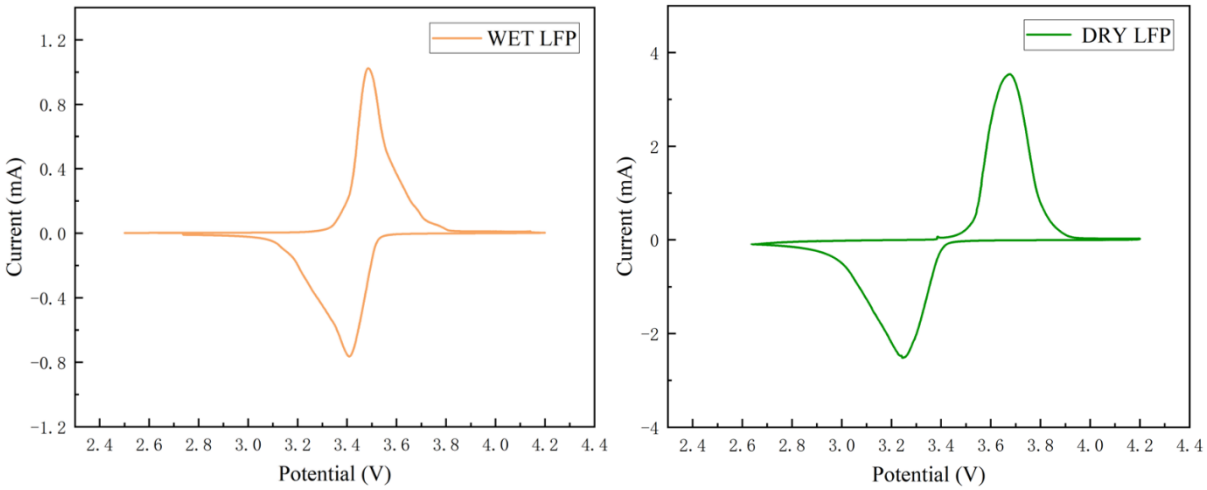

Figure 33: CV curves of LFP electrode, scanning from 2.5 V to 4.2 V, with a scanning rate of 0.1 mV/s.

NMC Electrode

NMC electrodes show a different scenario (in **Figure 34**). For the wet coating NMC electrode, the CV image exhibits a strange dumbbell shape. The inception of oxidation reaction occurs at 3.42 V, which is also close to the "symmetry center". The oxidation peak and reduction peak appear at 3.94 V and 2.95 V, respectively. And its peak current is also much lower than that of the wet coating LFP electrode. It is speculated that the reason for this phenomenon is the low activity of NMC811 under wet conditions. But the dry coating NMC electrode shows a more standard curve closer to that reported by the academic community (Wan and Chen, 2020). The dry coating NMC electrode began to undergo oxidation reaction at 3.56 V and reached a peak current of 2.53 mA at 3.85 V. Subsequently, as diffusion dominates the entire reaction, the current drops rapidly to 1.70 mA between 3.85 V and 3.97 V, but still maintains a high current value until the termination voltage of 4.2 V. This is due to the wide voltage window of the NMC811, which means it can still react and provide capacity at voltages up to 4.8 V (Savina and Abakumov, 2023). During the backward scanning, the first reduction peak appeared at 3.91 V with a peak current of -1.08 mA, and the second reduction peak, which was also the maximum reduction peak, appeared at 3.63 V with a current of -1.06 mA. More than one peak means that not only one reaction was taking place. The greater oxidation peak current than the reduction peak current suggests that NMC811 has a stronger oxidation activity.

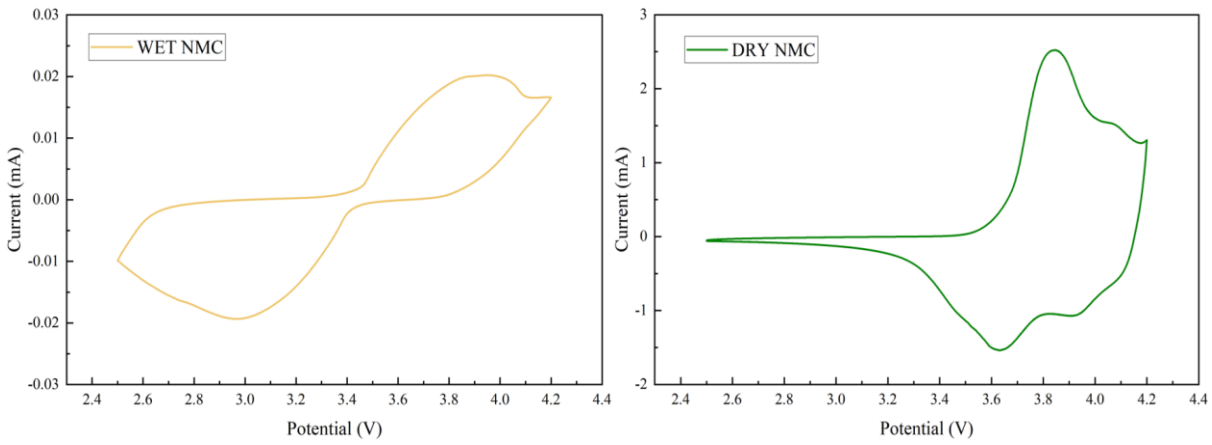

Figure 34: CV curves of NMC electrode, scanning from 2.5 V to 4.2 V, with a scanning rate of 0.1 mV/s.

LFP/NMC Blended Electrode

The LFP/NMC blended electrode exhibits a similar situation to the NMC electrode (as shown in **Figure 35**). For the blended electrode prepared by the wet coating process, the CV curve shows a high similarity to the NMC wet coating electrode. This means the activity of the NMC particles receives suppression in the wet coating and controls the overall chemical reaction. In contrast, the dry coating blended electrode presents a combination of characteristics of both LFP and NMC. The first oxidation peak appears at 3.64 V with a current of 2.54 mA, and the second oxidation peak appears at 3.80 V with a current of 1.64 mA. At the scan cutoff voltage of 4.2 V, the electrode still exhibits a tendency to form a peak. The reverse scan process is very similar. The first significant reduction peak appears at 3.66 V and the current is -0.83 mA. The second reduction peak, which is also the highest reduction peak, appears at 3.24 V, with a peak current of -1.76 mA. It can be seen that due to the influence of LFP, its maximum oxidation peak and reduction peak both appear at the position adjacent to LFP. The multiple peaks that appear later at high voltage are mainly affected by NMC. The blended electrode prepared by the dry coating method exhibited better chemical activity and reaction reversibility.

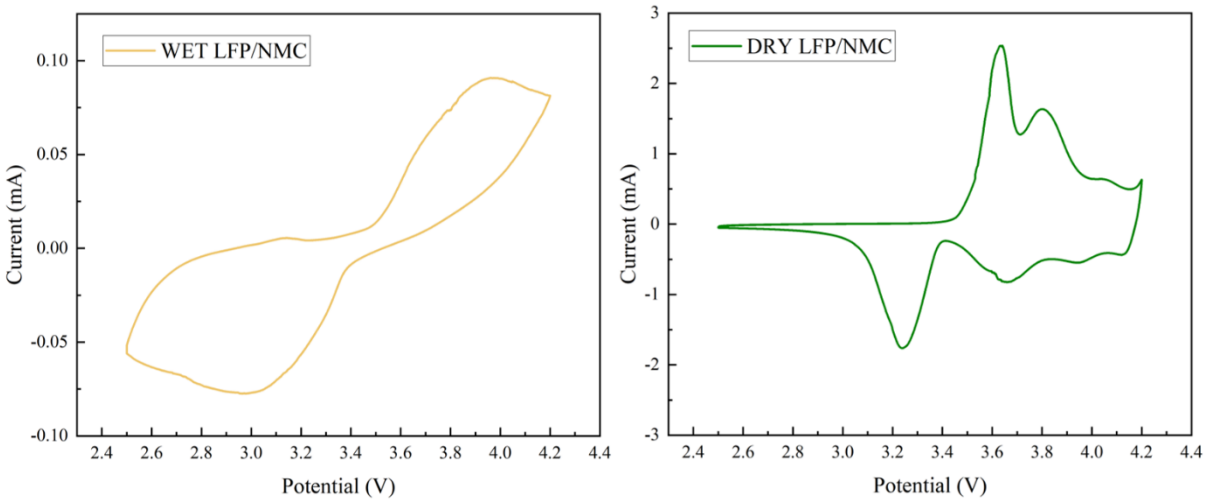

Figure 35: CV curves of LFP/NMC blended single-layer electrode, scanning from 2.5 V to 4.2 V, with a scanning rate of 0.1 mV/s.

5 Discussion

First, the designed serrated blade tool for the dry coating is addressed for discussion. Currently, the mainstream dry coating methods are PTFE fibrillation and electrospray technology. Both technologies place high demands on the technology and the operating environment. As presupposed, the designed solution should be simple, efficient, and economically viable to meet production needs. And the designed serrated blade method can perfectly match these. By using this tool, solid particle coatings with a thickness of around 1 mm can be prepared simply and efficiently, and a certain uniformity can be guaranteed. Different designs for the serration shape have been tried, such as the rectangle, but it would leave an obvious pattern. Therefore, a sufficiently sharp tip is required to ensure that as little pattern residue as possible remains. This triangular serration will ultimately leave only small scratches, which can be easily removed during the hot-pressing process. The circular pattern was not attempted, because the spacing between circles is difficult to adjust and can only be controlled by changing the radius. In addition, the spacing between adjacent circles may not be sufficient to allow particles to pass smoothly, thus causing blockage. In order to ensure that the tips of the serrations do not scrape the current collector, it is necessary to make sure that the tool is well supported and stiff enough. For large-scale applications, it is only necessary to widen the width of the tool to increase productivity per unit. By fixing this serrated blade on a moving conveyor belt, an automatic coating function can be achieved. It should be noted, however, that appropriate adjustments need to be made according to the characteristics of the solid material being added (e.g. particle size, and agglomeration properties).

To compare the wet coating and dry coating techniques, LFP electrode, NMC811 electrode, and LFP/NMC blended electrode were selected for the experiment. SEM observation of the electrode surfaces revealed that the wet coating LFP and NMC electrodes had more intact surfaces, whereas the dry coating electrode showed some small pores. The opposite result was obtained for the LFP/NMC blended electrode. The blended electrode prepared by the dry

coating had a smoother surface, while the wet method showed cracks distributed along the NMC particles. Such cracks can lead to inconsistencies in the charging and discharging process of the electrode material, affecting the diffusion process and leading to the deposition of inconsistent lithium dendrites, which is detrimental to the stability of the electrode. This explains why the dry coating blended electrode has a better performance in the later electrochemical performance tests. It is worth mentioning that the holes appearing on the surface of dry coating LFP and NNC electrodes are somewhat different from the cracks appearing in the blended electrodes, as the former does not lead to crack propagation under accumulated stress during reactions, thereby avoiding battery failure. Additionally, to a certain extent, having some voids on the surface is more favorable for electrolyte wetting and ion transport.

The cross-section images through SEM give the thickness of the electrodes prepared by the two methods. The thickness of the electrode prepared by the wet coating method is only 40 μm, while the electrode made by the dry coating method reaches 110 μm. Although their thickness both can be adjusted by adjusting the process parameters, the wet coating cannot produce very thick electrodes (hundreds of microns), while dry coating does not realize very thin electrodes (several microns). Therefore, it is challenging to control the thickness of electrodes prepared by the two methods to be consistent. However, the thickness of the electrode would have some influence on the electrolyte infiltration, lithium-ion diffusion, and charge transfer. This means that the experiment did not control the variables ideally. Because of this, the study of double-layer NMC electrodes was carried out later, which can serve as a supplement to the study of the effect of thickness on performance. In the process of preparing dry coating electrodes, it was an important issue to make a trade-off between the thickness and the density of electrodes. If the pressure of the calendering machine is too small, the thickness of the electrode will be too large, which is not beneficial to ion diffusion and the migration of electrons. But if the pressure is too high, the electrode will become very dense, the electrolyte will not be able to fully penetrate to the bottom, and the porosity of the electrode will become very low. This will

also result in a significant loss of battery performance. At least from the SEM results, the current parameters can not only ensure the integrity of the NMC particles, but also retain a certain number of pores so that the electrolyte and lithium ions have enough space to react and transport.

In the final electrochemical test, for the LFP electrode, these two methods demonstrated mostly consistent results. In cycling tests, the dry coating LFP electrode demonstrated a Coulomb efficiency of up to 99%, a specific capacity of 156.2 mAh/g close to the theoretical value, and an ultra-high capacity retention of 99.1% after 48 cycles. The LFP electrode prepared by the dry coating method has a higher specific capacity and capacity retention rate than the LFP electrode prepared by the wet coating method. However, this may be seen as a variance due to individual differences between electrodes. In subsequent rate capability tests and CV tests, they showed high consistency. However, for NMC materials, since the test results of different samples have a huge difference, it is difficult to draw a definite conclusion. The NMC electrode prepared by the dry coating method has a more stable performance. The “stable” here means that it has a smaller performance deviation in each sample. It is speculated that the activity of NMC811 particles in the solvent is inhibited, or that oxidation is caused by exposure to air for too long, which makes the wet coating NMC electrode have a lower capacity value, and the strange CV curve can also support this. This uncertainty is indicative of the fact that NMC materials are more sensitive and susceptible to processing parameters in a wet coating process. The fact that NMC811 has a higher capacity value and poor cycling stability than LFP was successfully observed in this experiment. Even though the dry coating LFP/NMC blended electrode exhibits better rate performance than the wet coating blended electrode, its stability cannot be guaranteed compared with the pure LFP or NMC electrode. Both the single-layer and double-layer electrodes failed after about 40 cycles. This shows that the mixing of LFP and NMC materials does not work well because they have different operating voltages, charging and discharging profiles. From a microscopic perspective, a plausible explanation is that the crystal structures of the two are not very compatible, causing the lattice to collapse when

lithium ions move between the lattices. This also explains why electric vehicle companies are currently focusing on mixing modules of LFP and NMC battery packs rather than direct material mixing of these two.

6 Conclusion

In this work, the dry coating process of electrodes is successfully simplified by designing a special blade tool with triangular serrations, which is promising for efficient, cost-effective dry coating process. The electrodes of LFP, NMC811, and LFP/NMC blended electrodes fabricated by wet coating and dry coating methods were compared. At the same time, NMC LFP double-layer electrodes made by dry coating have also been experimented as an innovative strategy. The SEM images show that the thickness of the single-layer electrode by wet coating is 40 μm, and its loading is about 1-2 mg (only active material), while the thickness of the electrode prepared by the dry coating method is about 110 μm, with a loading of 10-15 mg. The NMC LFP double-layer electrode made by dry coating has a loading of around 30 mg and a thickness of around 240 μm. For LFP and NMC electrodes, the wet coating electrodes have a smoother surface. However, for LFP/NMC blended electrodes, the opposite conclusion is drawn, and cracks along the NMC particles are observed on the surface of the wet coating LFP/NMC blended electrodes. In the final electrochemical performance characterization, the LFP electrode demonstrated high consistency across both methods. In contrast, the NMC electrodes of different samples showed a large variation in performance under wet coating conditions, which could be attributed to the oxidation of NMC due to prolonged exposure to air and solvents during wet processing. The NMC electrodes prepared by the dry method, on the other hand, have a small performance deviation. Ultimately, the wet coating LFP/NMC blended electrode performed poorly in both cycling and rate capacity tests due to the presence of surface cracks. Although the blended electrode prepared by the dry coating method obtained more acceptable results in the rate capacity test, also showed instability in the long cycling test. The NMC LFP double-layer electrode also did not show good stability. Therefore, it can be concluded that the mixing of LFP and NMC materials is not a good strategy. Combining the above performances and taking into account the low energy consumption, non-toxic properties and high production efficiency of dry coating technology, it can be considered that this is a very promising solution that may replace wet coating technology someday.

7 Future Work

In this work, due to time constraints, some data are not complete and perfect. For example, it is expected that the data of the long cycling test to be at least 100 cycles, yet in reality, only dozens of cycles are obtained. Therefore, the capacity retention rate of all batteries after 100 cycles was not obtained. Also in the CV test, neither the CV images of the wet coating NMC electrode nor the CV images of the wet coating LFP/NMC blended electrode obtained standard images similar to those from the dry coating method. Although many tests have been performed, it is still unclear whether this is due to individual differences in the fabrication process or a material defect. At the same time, the double-layer electrode can also be subjected to CV testing to compare with the single-layer structure to determine whether this layered structure is better than direct mixing. In addition, the double-layer structure tested in this experiment has NMC as the first layer, but a double-layer electrode structure with LFP as the first layer and NMC as the second layer can also be carried out. It is also a very important question whether the mixing of LFP and NMC can improve the thermal stability of the electrode, so thermal analysis tests can be studied in the future. Another important physical property is the adhesion of the electrodes. In the future, the electrodes prepared by both methods can be tested for adhesion to ensure that the electrode material can be firmly adhered to the collector without peeling off. It is worth mentioning that in this experiment, the thickness of the dry electrode and the wet electrode were not consistent. To ensure the rigor of the data, the thickness of the electrode needs to be controlled in future study.

References

Aryal, S. *et al.* (2021) ‘Roles of Mn and Co in Ni-rich layered oxide cathodes synthesized utilizing a Taylor Vortex Reactor’, *Electrochimica Acta*, 391, p. 138929. Available at: https://doi.org/10.1016/j.electacta.2021.138929.

Asenbauer, J. *et al.* (2020) ‘The success story of graphite as a lithium-ion anode material – fundamentals, remaining challenges, and recent developments including silicon (oxide) composites’, *Sustainable Energy & Fuels*, 4(11), pp. 5387–5416. Available at: https://doi.org/10.1039/D0SE00175A.

Bouguern, M.D. *et al.* (2024) ‘Engineering Dry Electrode Manufacturing for Sustainable Lithium-Ion Batteries’, *Batteries*, 10(1), p. 39. Available at: https://doi.org/10.3390/batteries10010039.

Bryntesen, S.N. *et al.* (2021) ‘Opportunities for the State-of-the-Art Production of LIB Electrodes—A Review’, *Energies*, 14(5), p. 1406. Available at: https://doi.org/10.3390/en14051406.

Chandra, G. *et al.* (2023) ‘Enhanced stability and high-yield LiFePO4/C derived from low-cost iron precursors for high-energy Li-ion batteries’, *Journal of Energy Storage*, 72, p. 108453. Available at: https://doi.org/10.1016/j.est.2023.108453.

Dallaev, R. *et al.* (2022) ‘Brief Review of PVDF Properties and Applications Potential’, *Polymers*, 14(22), p. 4793. Available at: https://doi.org/10.3390/polym14224793.

Deng, L. *et al.* (2022) ‘Recent Developments of Carbon-Based Anode Materials for Flexible Lithium-Ion Batteries’, *Crystals*, 12(9), p. 1279. Available at: https://doi.org/10.3390/cryst12091279.

Elgrishi, N. *et al.* (2018) ‘A Practical Beginner’s Guide to Cyclic Voltammetry’, *Journal of Chemical Education*, 95(2), pp. 197–206. Available at: https://doi.org/10.1021/acs.jchemed.7b00361.

e-motec (2022) ‘How Lithium Iron Phosphate Batteries Can Help Transform EVs’, *E-Motec*, 12 September. Available at: https://www.e-motec.net/lithium-iron-electric-mobility (Accessed: 11 June 2024).

Fichtner, M. *et al.* (2021) ‘Rechargeable Batteries of the Future—The State of the Art from a BATTERY 2030+ Perspective’, *Advanced Energy Materials*, 12, p. 2102904. Available at: https://doi.org/10.1002/aenm.202102904.

Goodenough, J.B. (2018) ‘How we made the Li-ion rechargeable battery’, *Nature Electronics*, 1(3), pp. 204–204. Available at: https://doi.org/10.1038/s41928-018-0048-6.

Gottschalk, L. *et al.* (2022) 'Improving the Performance of Lithium-Ion Batteries Using a Two-Layer, Hard Carbon-Containing Silicon Anode for Use in High-Energy Electrodes', *Energy Technology*, 11. Available at: https://doi.org/10.1002/ente.202200858.

Gyulai, A., Bauer, W. and Ehrenberg, H. (2023) 'Dry Electrode Manufacturing in a Calender: The Role of Powder Premixing for Electrode Quality and Electrochemical Performance', *ACS Applied Energy Materials*, 6(10), pp. 5122–5134. Available at: https://doi.org/10.1021/acsaem.2c03755.

Hebert, A. and Mccalla, E. (2021) 'The role of metal substitutions in the development of Li batteries, part I: Cathodes', *Materials Advances*, 2. Available at: https://doi.org/10.1039/D1MA00081K.

Hossain, Md.H. *et al.* (2023) 'Advances of lithium-ion batteries anode materials—A review', *Chemical Engineering Journal Advances*, 16, p. 100569. Available at: https://doi.org/10.1016/j.ceja.2023.100569.

Howard, I. *et al.* (2019) 'Coated and Printed Perovskites for Photovoltaic Applications', *Advanced Materials*, 31. Available at: https://doi.org/10.1002/adma.201806702.

Huang, K.-W. *et al.* (2024) 'Fast fabrication of μm-thick perovskite films by using a one-step doctor-blade coating method for direct X-ray detectors', *Journal of Materials Chemistry C*, 12(4), pp. 1533–1542. Available at: https://doi.org/10.1039/D3TC02736H.

Julien, C.M. *et al.* (2016) 'Olivine-Based Blended Compounds as Positive Electrodes for Lithium Batteries', *Inorganics*, 4(2), p. 17. Available at: https://doi.org/10.3390/inorganics4020017.

Kamarulzaman, N.H. *et al.* (2020) 'Optimization of Titanium Dioxide Layer Fabrication Using Doctor Blade Method in Improving Efficiency of Hybrid Solar Cells', *Journal of Physics: Conference Series*, 1535(1), p. 012025. Available at: https://doi.org/10.1088/1742-6596/1535/1/012025.

Khan, F.M.N.U. *et al.* (2023) 'Maximizing energy density of lithium-ion batteries for electric vehicles: A critical review', *Energy Reports*, 9, pp. 11–21. Available at: https://doi.org/10.1016/j.egyr.2023.08.069.

Kim, M.-H. *et al.* (2023) 'Design Strategies toward High-Performance Hybrid Carbon Bilayer Anode for Improved Ion Transport and Reaction Stability', *Advanced Functional Materials*, 33(3), p. 2208665. Available at: https://doi.org/10.1002/adfm.202208665.

Kotobuki, M., Yan, B. and Lu, L. (2023) 'Recent progress on cathode materials for rechargeable magnesium batteries', *Energy Storage Materials*, 54, pp. 227–253. Available at: https://doi.org/10.1016/j.ensm.2022.10.034.

Lienert, P. (2023) ‘Tesla 4680 battery’s secret sauce: Dry electrode coating’, *Reuters*, 10 March. Available at: https://www.reuters.com/technology/tesla-4680-batterys-secret-sauce-dry-electrode-coating-2023-03-10/ (Accessed: 4 April 2024).

Liu, T. *et al.* (2018) ‘Analysis of the relationship between vertical imparity distribution of conductive additive and electrochemical behaviors in lithium ion batteries’, *Electrochimica Acta*, 269, pp. 422–428. Available at: https://doi.org/10.1016/j.electacta.2018.03.038.

Liu, X. *et al.* (2021) ‘The Role of Cobalt and Manganese for the Safety of Ni-Rich NMC Cathode’, *ECS Meeting Abstracts*, MA2021-01(5), p. 304. Available at: https://doi.org/10.1149/MA2021-015304mtgabs.

Ludwig, B. *et al.* (2016a) ‘Solvent-Free Manufacturing of Electrodes for Lithium-ion Batteries’, *Scientific Reports*, 6(1), p. 23150. Available at: https://doi.org/10.1038/srep23150.

Ludwig, B. *et al.* (2016b) ‘Solvent-Free Manufacturing of Electrodes for Lithium-ion Batteries’, *Scientific Reports*, 6(1), p. 23150. Available at: https://doi.org/10.1038/srep23150.

Lung-Hao Hu, B. *et al.* (2013) ‘Graphene-modified LiFePO4 cathode for lithium ion battery beyond theoretical capacity’, *Nature Communications*, 4(1), p. 1687. Available at: https://doi.org/10.1038/ncomms2705.

Matthews, G. a. B. *et al.* (2024) ‘Solvent-free NMC electrodes for Li-ion batteries: unravelling the microstructure and formation of the PTFE nano-fibril network’, *Frontiers in Energy Research*, 11. Available at: https://doi.org/10.3389/fenrg.2023.1336344.

Morris C. (2023) *AM Batteries works with Amperex on solvent-free electrode manufacturing for Li-ion batteries*, *Charged EVs*. Available at: https://chargedevs.com/newswire/am-batteries-works-with-amperex-on-solvent-free-electrode-manufacturing-for-li-ion-batteries/ (Accessed: 8 April 2024).

Nitta, N. *et al.* (2015) ‘Li-ion battery materials: present and future’, *Materials Today*, 18(5), pp. 252–264. Available at: https://doi.org/10.1016/j.mattod.2014.10.040.

Reddy, M.V. *et al.* (2020) ‘Brief History of Early Lithium-Battery Development’, *Materials*, 13(8), p. 1884. Available at: https://doi.org/10.3390/ma13081884.

Reynolds, C.D. *et al.* (2021) ‘A review of metrology in lithium-ion electrode coating processes’, *Materials & Design*, 209, p. 109971. Available at: https://doi.org/10.1016/j.matdes.2021.109971.

Ryu, M. *et al.* (2023) ‘Ultrahigh loading dry-process for solvent-free lithium-ion battery electrode fabrication’, *Nature Communications*, 14(1), p. 1316. Available at: https://doi.org/10.1038/s41467-023-37009-7.

Savina, A.A. and Abakumov, A.M. (2023) ‘Benchmarking the electrochemical parameters of the LiNi0.8Mn0.1Co0.1O2 positive electrode material for Li-ion batteries’, *Heliyon*, 9(12), p. e21881. Available at: https://doi.org/10.1016/j.heliyon.2023.e21881.

Schalenbach, M. *et al.* (2023) ‘Ionic transport modeling for liquid electrolytes - Experimental evaluation by concentration gradients and limited currents’, *Electrochemical Science Advances*, 3(2), p. e2100189. Available at: https://doi.org/10.1002/elsa.202100189.

Sukenik, E.G., Kasaei, L. and Amatucci, G.G. (2023) ‘Impact of gradient porosity in ultrathick electrodes for lithium batteries’, *Journal of Power Sources*, 579, p. 233327. Available at: https://doi.org/10.1016/j.jpowsour.2023.233327.

Thapa, A.K. *et al.* (2022) ‘Mn-Rich NMC Cathode for Lithium-Ion Batteries at High-Voltage Operation’, *Energies*, 15(22), p. 8357. Available at: https://doi.org/10.3390/en15228357.

Vidal Laveda, J. *et al.* (2019) ‘Stabilizing Capacity Retention in NMC811/Graphite Full Cells via TMSPi Electrolyte Additives’, *ACS Applied Energy Materials*, 2(10), pp. 7036–7044. Available at: https://doi.org/10.1021/acsaem.9b00727.

Waldersee V. (2023) ‘VW masters dry-coating battery process with potential to slash cell costs’, *Reuters*, 16 June. Available at: https://www.reuters.com/business/autos-transportation/vw-masters-dry-coating-battery-process-with-potential-slash-cell-costs-2023-06-16/ (Accessed: 4 April 2024).

Wan, H. *et al.* (2023) ‘Interface design for all-solid-state lithium batteries’, *Nature*, 623(7988), pp. 739–744. Available at: https://doi.org/10.1038/s41586-023-06653-w.

Wan, S. and Chen, S. (2020) ‘A dithiol-based new electrolyte additive for improving electrochemical performance of NCM811 lithium ion batteries’, *Ionics*, 26(12), pp. 6023–6033. Available at: https://doi.org/10.1007/s11581-020-03768-2.

Wang, M. *et al.* (2020) ‘Effects of the Mixing Sequence on Making Lithium Ion Battery Electrodes’, *Journal of The Electrochemical Society*, 167(10), p. 100518. Available at: https://doi.org/10.1149/1945-7111/ab95c6.

Wang, X. *et al.* (2023) ‘A Polytetrafluoroethylene-Based Solvent-Free Procedure for the Manufacturing of Lithium-Ion Batteries’, *Materials*, 16(22), p. 7232. Available at: https://doi.org/10.3390/ma16227232.

Xue, Z. *et al.* (2023) ‘Research on the assembly process of full coin cells: key factors affecting data reliability’, *Ionics*, 29(12), pp. 5285–5293. Available at: https://doi.org/10.1007/s11581-023-05225-2.

Yao, W. *et al.* (2023) ‘A 5 V-class cobalt-free battery cathode with high loading enabled by dry coating’, *Energy & Environmental Science*, 16(4), pp. 1620–1630. Available at: https://doi.org/10.1039/D2EE03840D.

Yuan, W. *et al.* (2019) ‘Honeycomb-Inspired Surface-Patterned Cu@CuO Composite Current Collector for Lithium-Ion Batteries’, *Energy Technology*, 7(9), p. 1900445. Available at: https://doi.org/10.1002/ente.201900445.

Zhang, L. *et al.* (2021) ‘Carbon Anode Materials: A Detailed Comparison between Na-ion and K-ion Batteries’, *Advanced Energy Materials*, 11(11), p. 2003640. Available at: https://doi.org/10.1002/aenm.202003640.

Zhang, Y. *et al.* (2021) ‘A Review of Lithium-Ion Battery Electrode Drying: Mechanisms and Metrology’, *Advanced Energy Materials*, 12, p. 2102233. Available at: https://doi.org/10.1002/aenm.202102233.

Zhang, Y.S. *et al.* (2022) ‘A Review of Lithium-Ion Battery Electrode Drying: Mechanisms and Metrology’, *Advanced Energy Materials*, 12(2), p. 2102233. Available at: https://doi.org/10.1002/aenm.202102233.

Zhao, C. *et al.* (2023) ‘Modeling and Analysis of the Drying Process of Lithium-Ion Battery Electrodes Based on Non-Steady-State Drying Kinetics’, *Processes*, 11(11), p. 3236. Available at: https://doi.org/10.3390/pr11113236.

Zhou, H. *et al.* (2020) ‘Dense integration of solvent-free electrodes for Li-ion supercabattery with boosted low temperature performance’, *Journal of Power Sources*, 473, p. 228553. Available at: https://doi.org/10.1016/j.jpowsour.2020.228553.